

Non-Asymptotic Guarantees for Robust Identification of Granger Causality via the LASSO

Proloy Das, *Student Member, IEEE*, and Behtash Babadi, *Member, IEEE*

Abstract

Granger causality is among the widely used data-driven approaches for causal analysis of time series data with applications in various areas including economics, molecular biology, and neuroscience. Two of the main challenges of this methodology are: 1) over-fitting as a result of limited data duration, and 2) correlated process noise as a confounding factor, both leading to errors in identifying the causal influences. Sparse estimation via the LASSO has successfully addressed these challenges for parameter estimation. However, the classical statistical tests for Granger causality resort to asymptotic analysis of ordinary least squares, which require long data durations to be useful and are not immune to confounding effects. In this work, we close this gap by introducing a LASSO-based statistic and studying its non-asymptotic properties under the assumption that the true models admit sparse autoregressive representations. We establish that the sufficient conditions of LASSO also suffice for robust identification of Granger causal influences. We also characterize the false positive error probability of a simple thresholding rule for identifying Granger causal effects. We present simulation studies and application to real data to compare the performance of the ordinary least squares and LASSO in detecting Granger causal influences, which corroborate our theoretical results.

Index Terms

Granger Causality, LASSO, autoregressive models, non-asymptotic analysis.

I. INTRODUCTION

Reliable identification of causal influences is one of the central challenges in time series analysis, with implications for various domains such as economics [1], neuroscience [2]–[4] and computational biology [5], [6]. Granger causal (GC) characterization of time series is among the widely used methods in this regard. This framework was pioneered by Granger [7], with subsequent key generalizations provided by Geweke [8], [9]. The notion of GC influence pertains to assessing the improvements in predicting the future samples of one time series by incorporating the past samples of another one.

P. Das is with the Department of Anesthesiology, Critical Care and Pain Medicine, Massachusetts General Hospital, Boston, MA, 02114 USA (e-mail: pdas6@mgh.harvard.edu).

B. Babadi is with the Department of Electrical and Computer Engineering, University of Maryland, College Park, MD, 20742 USA (e-mail: behtash@umd.edu).

This work was supported by the National Science Foundation Awards No. 1552946 and 1807216 (Corresponding author: Proloy Das).

While causality, as the relationship between cause and effect, is a philosophically well-defined concept, it eludes a universal definition in empirical sciences and engineering. Granger causality is one of many definitions used in time series models (see [10], [11] for other notions), with an explicit data-driven form that admits statistical testing. The stochastic nature of the time series model, i.e., the uncertainty and the direction of time flow are the central features of GC definition. In principle, given two time series x_t and y_t , one asserts that y_t has a GC influence on x_t when the posterior densities $p(x_t|x_{t-1}, x_{t-2}, \dots, y_{t-1}, y_{t-2}, \dots)$ and $p(x_t|x_{t-1}, x_{t-2}, \dots)$ differ significantly. However, estimating these posterior densities from the observed data is a difficult task in general, and requires additional modeling assumptions. A popular set of such assumptions pertains to parametric multivariate autoregressive (MVAR) models along with certain distributional specifications (e.g., zero-mean Gaussian process noise). In these models, the aforementioned posterior densities can be fully characterized by the estimates of parameters and prediction error variances. As a consequence, one first aims at predicting x_{t+1} by a linear combination of the joint past observations $\{x_t, \dots, x_0\}$, $\{y_t, \dots, y_0\}$ (i.e., the *full* model), followed by repeating this task by excluding the past observations of y_t (i.e., the *reduced* model). If the prediction error variance in the former case is significantly smaller than the latter, we say that y_t has a GC influence on x_t .

Conventionally, the optimal linear predictors are obtained by the ordinary least squares (OLS), and the model orders are determined by the AIC [12] or BIC [13] procedures. Then, the GC measure is defined as the logarithmic ratio of the two prediction error variances, and its statistical significance is assessed based on the corresponding asymptotic distributions [14]–[16]. While the aforementioned procedure is relatively simple to carry out, it faces two key challenges. First, in order to obtain reliable MVAR parameter estimates via OLS, a relatively long observation horizon is required. In datasets with small sample size (e.g., gene expression data [17]), the regression models typically over-fit the observed data, causing both parameter estimation and model order selection to break down [4], [18]. In addition, AIC/BIC may restrict the order of the MVAR in a way that the resulting model fails to capture the complex and long-range dynamics of the underlying couplings [2], [19]. Secondly, correlated process noise arising from latent processes, may lead to misidentification of GC influences, which is often referred to as the confounding effect [20].

These challenges have been successfully addressed in the context of regularized MVAR estimation [21]–[29]. In particular, the theory of sparse estimation via the LASSO [30]–[33] provides a principled methodology for simultaneous parameter estimation and model selection in high dimensional MVAR models [22]–[27], [34]–[36]. In addition, the Oracle property of the LASSO in presence of correlated noise ensures robust recovery of the set of MVAR parameters arising from the direct causal influences while discarding any spurious couplings due to correlated process noise, thus alleviating the confounding effect. The LASSO and its variants have already been utilized in existing work to identify graphical GC influences based on the recovered sparsity patterns [37]–[42]. These methods construct the GC graph based on the estimated model parameters, either directly [37] or by appropriate thresholding [41], [42] to control false positive errors. This idea has even been extended to time series models that account for nonlinear dynamics using structured multilayer perceptrons or recurrent neural networks [43]. Another related class of results uses de-biasing techniques in order to construct confidence intervals and thereby identify the significant causal interactions [44]–[50]. There is, however, an evident disconnect between these LASSO-based approaches and

the classical OLS-based GC inference: while the LASSO-based approaches aim at identifying the GC effects based on consistent estimates of the parameters in the non-asymptotic regime, the classical GC methodology relies on the comparison of the prediction errors across the *full* and *reduced* models by resorting to asymptotic distributions.

In this paper, we close the gap between currently available LASSO-based approaches and the classical OLS-based GC inference by unifying these two approaches via introducing a new LASSO-based GC statistic that resembles the classical GC measure, and by leveraging the consistency properties of the LASSO to characterize the non-asymptotic properties of said GC statistic. In particular, we consider a canonical bivariate autoregressive (BVAR) process with correlated process noise. We then propose a likelihood-based scaled F-statistic as the relevant GC statistic, which we call the LGC statistic, and study its non-asymptotic properties under both the presence and absence of a GC influence. Our analysis reveals that the well-known sufficient conditions of the LASSO for stable BVAR estimation are also sufficient for accurate detection of the GC influences, if the strength of the causal effect satisfies additional mild conditions. Furthermore, by slightly weakening these sufficient conditions, we characterize the false positive error probability of a simple thresholding scheme for identification of GC influences.

We present simulation studies to compare the performance of the classical OLS-based and the proposed LGC-based approaches in detecting GC influences, in order to demonstrate the validity of our theoretical claims and to explore the key underlying trade-offs. We also present an application to experimentally-recorded neural data from general anesthesia to assess the causal role of the local field potential (LFP) on spiking activity. Our results based on LGC analysis corroborate existing hypotheses on the causal role of LFP in mediating local spiking activity, whereas these effects are concealed by the classical GC analysis due to significant over-fitting.

In summary, our main contribution is to extend the theoretical results of the LASSO to the classical characterization of GC influences, and to identify the key trade-offs in terms of sampling requirements and strength of the causal effects that result in robust GC identification. The rest of this paper is organized as follows: Section II provides background and our problem formulation. Our main theoretical contributions are given in Section III. Section IV presents application to simulated and experimentally-recorded neural data, followed by our concluding remarks in Section V.

II. BACKGROUND AND PROBLEM FORMULATION

A. Granger Causality in a Canonical BVAR Regression Model

Consider finite-duration observations from two time series x_t and y_t , given by $\{x_t, y_t\}_{t=-p+1}^n$, where n is the sample size and p is the order. The BVAR(p) model can be expressed as:

$$\begin{bmatrix} x_t \\ y_t \end{bmatrix} = \mathbf{A}_1 \begin{bmatrix} x_{t-1} \\ y_{t-1} \end{bmatrix} + \mathbf{A}_2 \begin{bmatrix} x_{t-2} \\ y_{t-2} \end{bmatrix} + \dots + \mathbf{A}_p \begin{bmatrix} x_{t-p} \\ y_{t-p} \end{bmatrix} + \begin{bmatrix} \epsilon_t \\ \epsilon'_t \end{bmatrix} \quad (1)$$

with $\mathbf{A}_i \in \mathbb{R}^{2 \times 2}$ for $i \in \{1, 2, \dots, p\}$ denoting the BVAR parameters and $[\epsilon_t, \epsilon'_t]^\top$ denoting the process noise with known distribution. It is commonly assumed that $[\epsilon_t, \epsilon'_t]^\top \sim \mathcal{N}(\mathbf{0}, \Sigma_\epsilon)$. Using this BVAR(p) model and considering $\{x_t, y_t\}_{t=-p+1}^0$ as the initial condition, one can form a prediction model of x_t as follows:

$$\mathbf{x} = \mathbf{X}\boldsymbol{\theta} + \boldsymbol{\epsilon}, \quad (2)$$

where the response \mathbf{x} , regressors \mathbf{X} , and residuals $\boldsymbol{\epsilon}$ are defined as:

$$\mathbf{x} = \begin{bmatrix} x_n \\ x_{n-1} \\ \vdots \\ x_1 \end{bmatrix}, \quad \mathbf{X} = \begin{bmatrix} x_{n-1} & \cdots & x_{n-p} & y_{n-1} & \cdots & y_{n-p} \\ x_{n-2} & \cdots & x_{n-p-1} & y_{n-2} & \cdots & y_{n-p-1} \\ \vdots & \cdots & \vdots & \vdots & \cdots & \vdots \\ x_0 & \cdots & x_{-p+1} & y_0 & \cdots & y_{-p+1} \end{bmatrix}, \quad \boldsymbol{\epsilon} = \begin{bmatrix} \epsilon_n \\ \epsilon_{n-1} \\ \vdots \\ \epsilon_1 \end{bmatrix}. \quad (3)$$

The regression coefficients $\boldsymbol{\theta}$ consist of $2p$ parameters: $\{\theta_i\}_{i=1}^p$, representing the autoregression coefficients obtained from $(\mathbf{A}_i)_{1,1}$, $i = 1, 2, \dots, p$ and $\{\theta_i\}_{i=p+1}^{2p}$ representing the cross-regression coefficients obtained from $(\mathbf{A}_i)_{1,2}$, $i = 1, 2, \dots, p$. Hereafter, we denote the true coefficients by $\boldsymbol{\theta}^* \in \mathbb{R}^{2p}$. Also, for a generic coefficient vector $\boldsymbol{\theta} \in \mathbb{R}^{2p}$, the corresponding auto- and cross-regression components are denoted by $\boldsymbol{\theta}_{(1)} \in \mathbb{R}^p$ and $\boldsymbol{\theta}_{(2)} \in \mathbb{R}^p$, respectively, i.e., $\boldsymbol{\theta} = [\boldsymbol{\theta}_{(1)}; \boldsymbol{\theta}_{(2)}]$.

The GC influence of y_t on x_t can then be assessed via hypothesis testing, with the null hypothesis $H_{y \rightarrow x, 0} : \boldsymbol{\theta}_{(2)}^* = \mathbf{0}$. For testing, one considers the following BVAR(p) models:

$$\text{Full Model: } \mathbf{x} = \mathbf{X}\boldsymbol{\theta} + \boldsymbol{\epsilon}, \quad (4a)$$

$$\text{Reduced Model: } \mathbf{x} = \mathbf{X}\tilde{\boldsymbol{\theta}} + \tilde{\boldsymbol{\epsilon}}, \text{ with } \tilde{\boldsymbol{\theta}}_{(2)} = \mathbf{0}. \quad (4b)$$

In other words, in the *full* model, all columns of \mathbf{X} are used to estimate \mathbf{x} , but in the *reduced* model, only the first p columns are used. The conventional GC measure [9] is then defined as the logarithmic ratio of the residual variances: $\mathcal{F}_{y \rightarrow x} := \log(\text{var}(\tilde{\boldsymbol{\epsilon}})/\text{var}(\boldsymbol{\epsilon}))$. Note that when the residuals are Gaussian, $\mathcal{F}_{y \rightarrow x}$ is the log-likelihood ratio statistic. Given that the *reduced* model is nested within the *full* model, we have $\mathcal{F}_{y \rightarrow x} \geq 0$.

In order to compute $\mathcal{F}_{y \rightarrow x}$ from the time series data, empirical residual variances are used based on OLS parameter estimates under both models [1]:

$$\hat{\boldsymbol{\theta}}_{\text{OLS}} = \underset{\boldsymbol{\theta}}{\text{argmin}} \frac{1}{n} \|\mathbf{x} - \mathbf{X}\boldsymbol{\theta}\|^2, \quad (5a)$$

$$\hat{\tilde{\boldsymbol{\theta}}}_{\text{OLS}} = \underset{\boldsymbol{\theta} : \boldsymbol{\theta}_{(2)} = \mathbf{0}}{\text{argmin}} \frac{1}{n} \|\mathbf{x} - \mathbf{X}\boldsymbol{\theta}\|^2. \quad (5b)$$

The estimated $\mathcal{F}_{y \rightarrow x}$ is a random variable over $\mathbb{R}_{\geq 0}$, and typically has a non-degenerate distribution. Thus, a non-zero $\mathcal{F}_{y \rightarrow x}$ does not necessarily imply a GC influence. To control for false discoveries, the well-established results on the asymptotic normality of maximum likelihood estimators can be utilized: under mild assumptions, $n\mathcal{F}_{y \rightarrow x}$ converges in distribution to a chi-square χ_p^2 with degree p . In addition, under a sequence of local alternatives $H_{y \rightarrow x, 1}^n : \boldsymbol{\theta}_{(2)}^* = \boldsymbol{\delta}/\sqrt{n}$, for some constant vector $\boldsymbol{\delta}$, $n\mathcal{F}_{y \rightarrow x}$ converges in distribution to a non-central chi-square $\chi_p^2(\nu)$ with degree p and non-centrality $\nu > 0$ [15], [16]. These asymptotic results lead to a simple thresholding strategy: rejecting the null hypothesis if $\mathcal{F}_{y \rightarrow x}$ exceeds a fixed threshold. A key consideration in this framework is choosing the model order p . To this end, criteria such as the AIC [12] and BIC [13] are widely used to strike a balance between the variance accounted for and the number of coefficients to be estimated.

While the foregoing procedure works well in practice for large sample sizes, its performance sharply degrades as the sample size decreases. This performance degradation has two main reasons:

- 1) The regression models become under-determined and result in poor estimates of the parameters, and
- 2) The conventional model selection criteria fail to capture possible long-range temporal coupling of the underlying processes.

As a result, the classical GC measure is highly susceptible to over-fitting. In addition, when the process noise elements ϵ_t and ϵ'_t are highly correlated, the OLS estimates incur additional error in capturing the true BVAR parameters, and hence result in mis-detection of the GC influences. While some existing nonparametric methods aim at entirely bypassing MVAR estimation by utilizing spectral matrix factorization [51] or multivariate embedding [52] for system identification, they are similarly prone to the adverse effects of small sample size. It is noteworthy that there also exists a slew of partial correlation-based nonparametric methods that employ conditional independence tests for causality detection [53]–[55], thus avoiding time series modeling assumptions altogether.

B. LASSO-based Causal Inference in the High-Dimensional Setting

In the so-called high-dimensional setting, where the model dimension becomes comparable to or even exceeds the sample size, regularization schemes are employed to guard against over-fitting. These schemes include Tikonov regularization [56], [57], ℓ_1 -regularization or the LASSO [30]–[33], smoothly clipped absolute deviation [58], [59], Elastic-Net [60], and their variants, and have particularly proven useful in MVAR estimation [21]–[24], [28], [29]. Among these techniques, the LASSO has been widely used and studied in the high-dimensional sparse MVAR setting, under fairly general assumptions [22]–[24]. By augmenting the least squares error loss with the ℓ_1 -norm of the parameters, the LASSO simultaneously guards against over-fitting and provides automatic model selection [33]–[36], [61], [62], under the hypothesis that the true parameters are sparse. In the context of MVAR estimation, assuming that the time series data admit a sparse MVAR representation, the LASSO estimates enjoy tight bounds on the estimation and prediction errors under suitable sample size requirements, even for models with correlated noise [26], [27].

By leveraging the foregoing properties, the LASSO and its variants have been utilized in existing work to identify GC influences in a graphical fashion [37]–[42]. These approaches construct the GC graph either directly from the estimated coefficients (e.g., [37]) or by appropriate thresholding (e.g., [41], [42]) to control false positive errors. Alternatively, de-biasing techniques have been introduced for constructing confidence intervals over the estimated parameters and thereby identifying the significant causal effects [44]–[50].

C. Unifying the Classical OLS-based and LASSO-based Approaches

Comparing the classical OLS-based and the recent LASSO-based approaches to causal inference reveals an evident disconnect: the latter approach directly utilizes the estimated parameters in a single model to identify the GC influence with non-asymptotic performance guarantees, while the former is based on comparing the prediction performance of two different models by resorting to asymptotic distributions for statistical testing.

Our main goal here is to close this gap by unifying these two approaches. To this end, we first replace OLS estimation in (5b) by its LASSO counterpart:

$$\hat{\theta} = \underset{\theta}{\operatorname{argmin}} \frac{1}{n} \|\mathbf{x} - \mathbf{X}\theta\|^2 + \lambda_n \|\theta\|_1 \quad (6a)$$

$$\widehat{\boldsymbol{\theta}} = \underset{\boldsymbol{\theta}: \boldsymbol{\theta}_{(2)} = \mathbf{0}}{\operatorname{argmin}} \frac{1}{n} \|\mathbf{x} - \mathbf{X}\boldsymbol{\theta}\|^2 + \lambda_n \|\boldsymbol{\theta}\|_1, \quad (6b)$$

where λ_n denotes the regularization parameter. Let

$$\ell(\boldsymbol{\theta}_{(1)}, \boldsymbol{\theta}_{(2)}) := \frac{1}{n} \|\mathbf{x} - \mathbf{X}\boldsymbol{\theta}\|^2 \text{ with } \boldsymbol{\theta} = [\boldsymbol{\theta}_{(1)}; \boldsymbol{\theta}_{(2)}].$$

By similarly grouping the solutions of (6) as $\widehat{\boldsymbol{\theta}} = [\widehat{\boldsymbol{\theta}}_{(1)}; \widehat{\boldsymbol{\theta}}_{(2)}]$ and $\widetilde{\boldsymbol{\theta}} = [\widetilde{\boldsymbol{\theta}}_{(1)}; \mathbf{0}]$, we then propose to use the following statistic:

$$\mathcal{T}_{y \rightarrow x} := \frac{\ell(\widetilde{\boldsymbol{\theta}}_{(1)}, \mathbf{0})}{\ell(\widehat{\boldsymbol{\theta}}_{(1)}, \widehat{\boldsymbol{\theta}}_{(2)})} - 1 = \frac{\ell(\widetilde{\boldsymbol{\theta}}_{(1)}, \mathbf{0}) - \ell(\widehat{\boldsymbol{\theta}}_{(1)}, \widehat{\boldsymbol{\theta}}_{(2)})}{\ell(\widehat{\boldsymbol{\theta}}_{(1)}, \widehat{\boldsymbol{\theta}}_{(2)})}, \quad (7)$$

akin to a scaled likelihood-based version of the F-statistic, which we call the LASSO-based GC (LGC) statistic. Note that the LGC statistic can be related to the conventional GC statistic as $\mathcal{T}_{y \rightarrow x} = \exp(\mathcal{F}_{y \rightarrow x}) - 1$, when $\lambda_n = 0$. Therefore, it is expected for $\mathcal{T}_{y \rightarrow x}$ to be near 0 under the null hypothesis. One advantage of using this statistic is that a simple thresholding strategy, similar to that used for the classical GC statistic, can be used to reject the null hypothesis $H_{y \rightarrow x, 0} : \boldsymbol{\theta}_{(2)}^* = \mathbf{0}$. In the next section, we will characterize the non-asymptotic properties of the LGC statistic and seek conditions that allow us to distinguish between the null (i.e., absence of a GC effect) and a suitably defined alternative (i.e., presence of a GC effect) hypothesis.

III. THEORETICAL RESULTS

Our main theoretical contribution in this section is to characterize $\mathcal{T}_{y \rightarrow x}$ under both the null and a suitably chosen alternative hypothesis, and establish sufficient conditions that guarantee distinguishing these hypotheses with high probability. We will also analyze the false positive error probability corresponding to the aforementioned thresholding strategy, under slightly weakened sufficient conditions. The latter result can be used to obtain suitable thresholds in practice, as we will demonstrate in Section IV. Before presenting the main results, we state our key assumptions and discuss their implications in the following section.

A. Key Assumptions and Their Implications

Following [26], we impose the following assumptions on the BVAR process:

Assumption 1. The $\{x_t, y_t\}_{t=-p+1}^n$ is a part of a realization of zero-mean bivariate process that admits a stable and invertible BVAR(p) representation, with a zero-mean i.i.d. Gaussian process noise with positive definite covariance Σ_ϵ . Further, the initial condition of the process is such that the samples under consideration attain the stationary distribution.

To elaborate on the implications of Assumption 1 for the second order statistics of the BVAR process, let $\boldsymbol{\Gamma}(l)$ be the auto-covariance matrix of the BVAR process at lag l and

$$\mathbf{F}(\omega) := \frac{1}{2\pi} \sum_{l=-\infty}^{\infty} \boldsymbol{\Gamma}(l) \exp(-il\omega)$$

be its spectral density matrix. It can be shown that the spectral density exists, if $\sum_{l=0}^{\infty} \|\boldsymbol{\Gamma}(l)\|_2^2 < \infty$. Furthermore, if $\sum_{l=0}^{\infty} \|\boldsymbol{\Gamma}(l)\|_2 < \infty$, the spectral density is bounded and continuous, so that the essential supremum is indeed

achieved. Hereafter, we denote the maximum and minimum eigen-values of any matrix \mathbf{M} by $\Lambda_{\max}(\mathbf{M})$ and $\Lambda_{\min}(\mathbf{M})$, respectively.

For the BVAR(p) process in (1), the matrix valued characteristic polynomial is defined as $\mathbf{A}(z) := \mathbf{I} - \sum_{j=1}^p \mathbf{A}_j z^j$. Then, the following consequences of Assumption 1 provide a simple characterization of the spectral density matrix:

- 1) The process noise covariance matrix Σ_ϵ is positive definite with bounded eigen-values, i.e.,

$$0 < \Lambda_{\min}(\Sigma_\epsilon) \leq \Lambda_{\max}(\Sigma_\epsilon) < \infty.$$

- 2) The BVAR process is stable and invertible, i.e., $\det(\mathbf{A}(z)) \neq 0$ on or inside the unit circle, $\{z \in \mathbb{C} : |z| \leq 1\}$.

Under these two conditions, the spectral density matrix exists, and its maximum eigen-value is bounded almost everywhere on $[-\pi, \pi]$, i.e.,

$$\mathcal{M}(\mathbf{F}) := \operatorname{ess\,sup}_{\omega \in [-\pi, \pi]} \Lambda_{\max}(\mathbf{F}(\omega)) < \infty.$$

Furthermore, it is bounded and continuous, and admits the representation:

$$\mathbf{F}(\omega) = \frac{1}{2\pi} \mathbf{A}^{-1}(\exp(-i\omega)) \Sigma_\epsilon \mathbf{A}^{-H}(\exp(-i\omega)).$$

Additionally, consider the infimum of the spectral density over unit circle:

$$m(\mathbf{F}) := \operatorname{ess\,inf}_{\omega \in [-\pi, \pi]} \Lambda_{\max}(\mathbf{F}(\omega)).$$

Then, the following useful bounds hold for the BVAR(p) process in (1):

$$\mathcal{M}(\mathbf{F}) \leq \frac{1}{2\pi} \frac{\Lambda_{\max}(\Sigma_\epsilon)}{\mu_{\min}(\mathbf{A})}, \quad m(\mathbf{F}) \geq \frac{1}{2\pi} \frac{\Lambda_{\min}(\Sigma_\epsilon)}{\mu_{\max}(\mathbf{A})}, \quad (8)$$

where $\mu_{\max}(\mathbf{A}) := \min_{|z|=1} \Lambda_{\max}(\mathbf{A}^H(z)\mathbf{A}(z))$ and $\mu_{\min}(\mathbf{A}) := \max_{|z|=1} \Lambda_{\min}(\mathbf{A}^H(z)\mathbf{A}(z))$.

We note that the characteristic polynomial $\mathbf{A}(z)$ encodes the temporal dependencies of the process, whereas Σ_ϵ captures the correlation between the process noise components, possibly due to latent processes. Expressing the error bounds in our theoretical analysis in terms of $\mu_{\max}(\mathbf{A})$, $\mu_{\min}(\mathbf{A})$, $\Lambda_{\max}(\Sigma_\epsilon)$, $\Lambda_{\min}(\Sigma_\epsilon)$, instead of $\mathcal{M}(\mathbf{F})$ and $m(\mathbf{F})$, helps to distinguish the contributions of these two sources of BVAR dependencies (See Appendix A).

We also consider the $2p$ -dimensional alternative BVAR(1) representation of the 2-dimensional BVAR(p) process: $\mathbf{X}_t = \check{\mathbf{A}}_1 \mathbf{X}_{t-1} + \check{\epsilon}$, where \mathbf{X}_t is the first the row of \mathbf{X} in (3) organized as a column vector, and $\check{\mathbf{A}}_1$ and $\check{\epsilon}$ are constructed by the corresponding augmentation of \mathbf{A}_i 's and ϵ_t 's, respectively. The process \mathbf{X}_t has a characteristic polynomial, $\check{\mathbf{A}}(z) := \mathbf{I} - \check{\mathbf{A}}_1 z$ and is stable if and only if the original process is stable [63].

The remaining component of our key assumptions is the following sparsity assumption, frequently arising in high-dimensional regime, specially in LASSO literature.

Assumption 2. The regression coefficients in (2), θ^* is k -sparse, i.e., $\|\theta^*\|_0 = k$.

The implication of this assumption for the *full* model is fairly standard, under both the null and alternative hypotheses. However, for the *reduced* model under the alternative hypothesis, where only the autoregressive parameters are unspecified and the cross-regression parameters are enforced to be $\mathbf{0}$, we need to define a suitable surrogate ‘‘true’’ model. Let the columns of \mathbf{X} corresponding to $\theta_{(i)}$ be denoted by $\mathbf{X}_{(i)}$, for $i = 1, 2$. To this end,

we use the orthogonality principle to define the surrogate “true” autoregression coefficients in the *reduced* model as:

$$\tilde{\boldsymbol{\theta}}_{(1)}^* := \boldsymbol{\theta}_{(1)}^* + \mathbf{C}_{11}^{-1} \mathbf{C}_{12} \boldsymbol{\theta}_{(2)}^*,$$

where

$$\mathbb{E} \left[\frac{1}{n} \mathbf{X}^\top \mathbf{X} \right] = \begin{bmatrix} \mathbb{E} \left[\frac{1}{n} \mathbf{X}_{(1)}^\top \mathbf{X}_{(1)} \right] & \mathbb{E} \left[\frac{1}{n} \mathbf{X}_{(1)}^\top \mathbf{X}_{(2)} \right] \\ \mathbb{E} \left[\frac{1}{n} \mathbf{X}_{(2)}^\top \mathbf{X}_{(1)} \right] & \mathbb{E} \left[\frac{1}{n} \mathbf{X}_{(2)}^\top \mathbf{X}_{(2)} \right] \end{bmatrix} =: \begin{bmatrix} \mathbf{C}_{11} & \mathbf{C}_{12} \\ \mathbf{C}_{21} & \mathbf{C}_{22} \end{bmatrix} =: \mathbf{C}.$$

Note that even though the MVAR coefficients under the alternative hypothesis are k -sparse, the surrogate “true” autoregression coefficients under the *reduced* model may not be. To deal with this issue, we follow the treatment of [32] in analyzing the LASSO under weakly sparse or compressible parameters, and further impose a norm condition on $\boldsymbol{\theta}_{(2)}^*$ (See the statement of Theorem 1) to restrict the alternative hypothesis. The latter ensures that the *full* and *reduced* models are distinguishable under the alternative hypothesis.

B. Main Theoretical Results

Our main theorem is stated as follows:

Theorem 1 (Main Theorem). *Suppose that the key assumptions 1 and 2 hold. Then, for the proposed LGC statistic $\mathcal{T}_{y \rightarrow x}$ evaluated at the BVAR(p) parameter estimates from the solutions of (6) with a regularization parameter $\lambda_n = 4\mathcal{A}\sqrt{\log(2p)/n}$, there exists a threshold that correctly distinguishes the null and the local alternative hypothesis $H_{y \rightarrow x,1}^n : \|\boldsymbol{\theta}_{(2)}^*\|_2^2 \geq \mathcal{B}k \log(2p)/n$ with probability at least $1 - K_1 \exp(-n\bar{c}) - K_2/p^{\bar{d}}$, if $n \geq \max\{\mathcal{C}'', \mathcal{D}''k\} \log(2p)$, with \mathcal{A} , \mathcal{B} , \mathcal{C}'' , \mathcal{D}'' , K_1 , K_2 , \bar{c} , and $\bar{d} > 0$ denoting constants that are explicitly given in the proof.*

Proof. The proof has three main steps. First, we bound the deviation of the empirical quantities $\ell(\widehat{\boldsymbol{\theta}}_{(1)}, \widehat{\boldsymbol{\theta}}_{(2)})$ (*full* model) and $\ell(\widehat{\boldsymbol{\theta}}_{(1)}, \mathbf{0})$ (*reduced* model) with respect to their counterparts evaluated at the true parameters. After invoking suitable concentration results for $\ell(\boldsymbol{\theta}_{(1)}^*, \boldsymbol{\theta}_{(2)}^*)$ and $\ell(\widehat{\boldsymbol{\theta}}_{(1)}^*, \mathbf{0})$, we can then lower bound $\mathcal{T}_{y \rightarrow x}$ under the alternative hypothesis and upper bound it under the null hypothesis. Secondly, we seek conditions under which the bounds do not coincide, which further restricts the alternative hypothesis. The last step of the proof establishes that these deviation and concentration results indeed hold with high probability.

Step 1. We first assume the deviation bounds:

$$\left| \ell(\widehat{\boldsymbol{\theta}}_{(1)}, \widehat{\boldsymbol{\theta}}_{(2)}) - \ell(\boldsymbol{\theta}_{(1)}^*, \boldsymbol{\theta}_{(2)}^*) \right| \leq \Delta_F, \quad (9)$$

$$\left| \ell(\widehat{\boldsymbol{\theta}}_{(1)}, \mathbf{0}) - \ell(\tilde{\boldsymbol{\theta}}_{(1)}^*, \mathbf{0}) \right| \leq \Delta_R, \quad (10)$$

and the concentration inequities:

$$\left| \ell(\boldsymbol{\theta}_{(1)}^*, \boldsymbol{\theta}_{(2)}^*) - (\boldsymbol{\Sigma}_\epsilon)_{1,1} \right| \leq \Delta_N \quad (11)$$

$$\left| \ell(\tilde{\boldsymbol{\theta}}_{(1)}^*, \mathbf{0}) - \ell(\boldsymbol{\theta}_{(1)}^*, \boldsymbol{\theta}_{(2)}^*) - D \right| \leq \Delta_D \quad (12)$$

hold for some non-negative quantities, Δ_F , Δ_R , Δ_N , Δ_D and $D := \boldsymbol{\theta}_{(2)}^* \top (\mathbf{C}_{22} - \mathbf{C}_{21} \mathbf{C}_{11}^{-1} \mathbf{C}_{12}) \boldsymbol{\theta}_{(2)}^*$. Using the bounds in (9) and (10), we get:

$$\frac{\ell(\tilde{\boldsymbol{\theta}}_{(1)}^*, \mathbf{0}) - \Delta_R}{\ell(\boldsymbol{\theta}_{(1)}^*, \boldsymbol{\theta}_{(2)}^*) + \Delta_F} \leq \frac{\ell(\tilde{\hat{\boldsymbol{\theta}}}_{(1)}, \mathbf{0})}{\ell(\tilde{\hat{\boldsymbol{\theta}}}_{(1)}, \tilde{\hat{\boldsymbol{\theta}}}_{(2)})} \leq \frac{\ell(\tilde{\boldsymbol{\theta}}_{(1)}^*, \mathbf{0}) + \Delta_R}{\ell(\boldsymbol{\theta}_{(1)}^*, \boldsymbol{\theta}_{(2)}^*) - \Delta_F}, \quad (13)$$

which gives the following lower and upper bounds on $\mathcal{T}_{y \rightarrow x}$:

$$\frac{\ell(\tilde{\boldsymbol{\theta}}_{(1)}^*, \mathbf{0}) - \ell(\boldsymbol{\theta}_{(1)}^*, \boldsymbol{\theta}_{(2)}^*) - \Delta_R - \Delta_F}{\ell(\boldsymbol{\theta}_{(1)}^*, \boldsymbol{\theta}_{(2)}^*) + \Delta_F} \leq \mathcal{T}_{y \rightarrow x} \leq \frac{\ell(\tilde{\boldsymbol{\theta}}_{(1)}^*, \mathbf{0}) - \ell(\boldsymbol{\theta}_{(1)}^*, \boldsymbol{\theta}_{(2)}^*) + \Delta_R + \Delta_F}{\ell(\boldsymbol{\theta}_{(1)}^*, \boldsymbol{\theta}_{(2)}^*) - \Delta_F}. \quad (14)$$

Now, under the null hypothesis $H_{y \rightarrow x, 0} : \boldsymbol{\theta}_{(2)} = \mathbf{0}$, we have $\ell(\tilde{\boldsymbol{\theta}}_{(1)}^*, \mathbf{0}) = \ell(\boldsymbol{\theta}_{(1)}^*, \boldsymbol{\theta}_{(2)}^*)$ and $\Delta_R = \Delta_F$, which implies:

$$\mathcal{T}_{y \rightarrow x} \leq \frac{\Delta_R + \Delta_F}{\ell(\boldsymbol{\theta}_{(1)}^*, \boldsymbol{\theta}_{(2)}^*) - \Delta_F} \leq \frac{2\Delta_F}{(\boldsymbol{\Sigma}_\epsilon)_{1,1} - \Delta_N - \Delta_F}, \quad (15)$$

with application of (11).

On the other hand, under a general alternative hypothesis $H_{y \rightarrow x, 0} : \boldsymbol{\theta}_{(2)}^* \neq \mathbf{0}$, (12) can be used to show that:

$$\mathcal{T}_{y \rightarrow x} \geq \frac{\ell(\tilde{\boldsymbol{\theta}}_{(1)}^*, \mathbf{0}) - \ell(\boldsymbol{\theta}_{(1)}^*, \boldsymbol{\theta}_{(2)}^*) - \Delta_R - \Delta_F}{\ell(\boldsymbol{\theta}_{(1)}^*, \boldsymbol{\theta}_{(2)}^*) + \Delta_F} \geq \frac{D - (\Delta_D + \Delta_R + \Delta_F)}{(\boldsymbol{\Sigma}_\epsilon)_{1,1} + \Delta_N + \Delta_F}. \quad (16)$$

From the upper and lower bounds in (15) and (16), it is possible to choose a threshold to distinguish between the two hypothesis without ambiguity, if:

$$\frac{D - (\Delta_D + \Delta_R + \Delta_F)}{(\boldsymbol{\Sigma}_\epsilon)_{1,1} + \Delta_N + \Delta_F} > \frac{2\Delta_F}{(\boldsymbol{\Sigma}_\epsilon)_{1,1} - \Delta_N - \Delta_F}, \quad (17)$$

which after rearrangement translates to:

$$D > \Delta_D + \Delta_R + \Delta_F \left(1 + 2 \frac{(\boldsymbol{\Sigma}_\epsilon)_{1,1} + \Delta_N + \Delta_F}{(\boldsymbol{\Sigma}_\epsilon)_{1,1} - (\Delta_N + \Delta_F)} \right). \quad (18)$$

Next, we choose $\Delta_N = (\boldsymbol{\Sigma}_\epsilon)_{1,1}/4$. Then, assuming $\Delta_F \leq (\boldsymbol{\Sigma}_\epsilon)_{1,1}/4$, the bound of (18) further simplifies to

$$D > \Delta_D + \Delta_R + 7\Delta_F. \quad (19)$$

Step 2. Next, we assume that the following conditions hold:

Condition 1 (Restricted eigenvalue (RE) condition). The symmetric matrix $\hat{\boldsymbol{\Sigma}} = \mathbf{X}^\top \mathbf{X}/n \in \mathbb{R}^{2p \times 2p}$ satisfies restricted eigenvalue condition with curvature $\alpha > 0$ and tolerance $\tau \geq 0$, i.e., $\hat{\boldsymbol{\Sigma}} \sim \text{RE}(\alpha, \tau)$:

$$\boldsymbol{\phi}^\top \hat{\boldsymbol{\Sigma}} \boldsymbol{\phi} \geq \alpha \|\boldsymbol{\phi}\|_2^2 - \tau \|\boldsymbol{\phi}\|_1^2, \quad \forall \boldsymbol{\phi} \in \mathbb{R}^{2p},$$

with

$$\tau := \frac{m-1}{m} \frac{\alpha}{32k}$$

for some constant $m > 1$.

Condition 2 (Deviation condition). There exist deterministic functions $\mathbb{Q}(\boldsymbol{\theta}^*, \boldsymbol{\Sigma}_\epsilon)$, $\mathbb{Q}'(\boldsymbol{\theta}^*, \boldsymbol{\Sigma}_\epsilon)$ such that

$$\left\| \frac{1}{n} \mathbf{X}^\top (\mathbf{x} - \mathbf{X}\boldsymbol{\theta}^*) \right\|_\infty \leq \mathbb{Q}(\boldsymbol{\theta}^*, \boldsymbol{\Sigma}_\epsilon) \sqrt{\frac{\log 2p}{n}},$$

$$\left\| \frac{1}{n} \mathbf{X}_{(1)}^\top (\mathbf{x} - \mathbf{X}_{(1)} \tilde{\boldsymbol{\theta}}_{(1)}^*) \right\|_\infty \leq \mathbb{Q}'(\boldsymbol{\theta}^*, \boldsymbol{\Sigma}_\epsilon) \sqrt{\frac{\log 2p}{n}}.$$

Under these conditions, we can use the expressions for the non-negative quantities, Δ_F , Δ_R and Δ_D derived in Propositions 1 and 2 (Appendix A) and Lemma 3 (Appendix C), respectively, to obtain the following bound on the right hand side of (19):

$$\Delta_D + \Delta_R + 7\Delta_F \leq a \sqrt{\frac{\log 2p}{n}} \|\boldsymbol{\theta}_{(2)}^*\|_2^2 + \flat \sqrt{\frac{k \log 2p}{n}} \|\boldsymbol{\theta}_{(2)}^*\|_2 + c \frac{k \log 2p}{n},$$

where

$$\begin{aligned} a &= \frac{\alpha}{27} \left(\|\mathbf{C}_{11}^{-1} \mathbf{C}_{12}\|_2^2 + 1 \right), \\ \flat &= \mathfrak{A} \left[\left(32\sqrt{2m} + 73 \right) \|\mathbf{C}_{11}^{-1} \mathbf{C}_{12}\| + 1 \right], \\ c &= \frac{16\mathfrak{A}^2}{\alpha/m} \left(\frac{168}{m+1} + 20 \right), \end{aligned}$$

provided the lasso problems are solved with the choice of $\lambda_n = 4\mathfrak{A} \sqrt{\log 2p/n}$, for \mathfrak{A} satisfying (See Propositions 6 and 7 in Appendix B):

$$\mathfrak{A} \geq \max \{ \mathbb{Q}(\boldsymbol{\theta}^*, \boldsymbol{\Sigma}_\epsilon), \mathbb{Q}'(\boldsymbol{\theta}^*, \boldsymbol{\Sigma}_\epsilon) \}.$$

Also, note that the assumption $\Delta_F \leq (\boldsymbol{\Sigma}_\epsilon)_{1,1}/4$ requires:

$$\frac{24}{m+1} \frac{k\lambda_n^2}{\alpha/m} \leq \frac{(\boldsymbol{\Sigma}_\epsilon)_{1,1}}{4}. \quad (20)$$

and imposes an upper bound on λ_n . The implications of this upper bound are further discussed in *Remark 2* at the end of this section.

Next, we use the following lower bound on D : $D \geq \tilde{\Lambda}_{\min} \|\boldsymbol{\theta}_{(2)}^*\|_2^2$, with $\tilde{\Lambda}_{\min} := \Lambda_{\min} (\mathbf{C}_{22} - \mathbf{C}_{21} \mathbf{C}_{11}^{-1} \mathbf{C}_{12})$, which gives the following sufficient condition for inequality (19) to hold:

$$\tilde{\Lambda}_{\min} \|\boldsymbol{\theta}_{(2)}^*\|_2^2 \geq a \sqrt{\frac{\log 2p}{n}} \|\boldsymbol{\theta}_{(2)}^*\|_2^2 + \flat \sqrt{\frac{k \log 2p}{n}} \|\boldsymbol{\theta}_{(2)}^*\|_2 + c \frac{k \log 2p}{n}. \quad (21)$$

By further requiring $n \geq \mathfrak{C}' \log(2p)$, where

$$\mathfrak{C}' = \left(\frac{2\alpha \left(\|\mathbf{C}_{11}^{-1} \mathbf{C}_{12}\|_2^2 + 1 \right)}{27\tilde{\Lambda}_{\min}} \right)^2,$$

we have $\tilde{\Lambda}_{\min} - a \sqrt{\log 2p/n} \geq \tilde{\Lambda}_{\min}/2$. The latter combined with (21), and an application of Lemma 4 (Appendix C) gives the sufficient condition: $\|\boldsymbol{\theta}_{(2)}^*\|_2^2 \geq \mathfrak{B} k \log 2p/n$ for unambiguous discrimination between the null and the local alternative hypothesis $H_{y \rightarrow x, 0}^n : \|\boldsymbol{\theta}_{(2)}^*\|_2^2 \geq \mathfrak{B} k \log 2p/n$, as long as $n \geq \max\{\mathfrak{C}', \mathfrak{D}' k\} \log(2p)$, where

$$\mathfrak{B} := \left(\frac{4\flat^2}{\tilde{\Lambda}_{\min}^2} + \frac{4c}{\tilde{\Lambda}_{\min}} \right), \text{ and } \mathfrak{D}' := \frac{1536m}{m+1} \frac{\mathfrak{A}^2}{\alpha(\boldsymbol{\Sigma}_\epsilon)_{1,1}}.$$

Note that the condition $n \geq \mathfrak{D}' k \log(2p)$ ensures the upper bound (20) on λ_n .

Step 3. It only remains to bound the probability of the event that the null and *local* alternative hypotheses are distinguishable. Proposition 5 (Appendix B) establishes that Condition 1 holds with probability at least

$$1 - c_1 \exp(-c_2 n \min\{\zeta^{-2}, 1\}), \quad (22)$$

if $n \geq C_0 \max\{\zeta^2, 1\} k \log 2p$, for some constants C_0, c_1, c_2 , and $\zeta (> 0)$. Also, Propositions 6 and 7 (Appendix B) establish that Condition 2 holds with probability at least

$$1 - \frac{d_1}{(2p)^{d_2}} - \frac{d'_1}{(2p)^{d'_2}}, \quad (23)$$

if $n \geq \max\{D_0, D'_0\} \log(2p)$, for some constants $d_1, d'_1, d_2, d'_2, D_0$, and $D'_0 (> 0)$.

From Lemma 2 (Appendix C), the first deviation bound (9) holds with probability $1 - 2 \exp(-n/128)$ with the choice $\Delta_N = (\Sigma_\epsilon)_{1,1}/4$. Lastly, from Lemma 3 (Appendix C), the deviation bound (9) holds with probability $1 - c_3 \exp(-c_4 n \min\{\zeta^{-2} \log 2p/n, 1\})$, under Condition 2.

Combining the two steps, the claim of the theorem holds with probability at least

$$1 - 2 \exp\left(-\frac{n}{128}\right) - c_1 \exp(-c_2 n \min\{\zeta^{-2}, 1\}) - c_3 \exp\left(-c_4 n \min\{\zeta^{-2} \max\{D_0, D'_0\}, 1\}\right) - \frac{d_1}{(2p)^{d_2}} - \frac{d'_1}{(2p)^{d'_2}}, \quad (24)$$

if $n \geq \max\{\mathcal{C}'', \mathcal{D}'' k\} \log(2p)$, where $\mathcal{D}'' := \max\{\mathcal{D}', C_0 \max\{\zeta^2, 1\}\}$ and $\mathcal{C}'' = \max\{\mathcal{C}', D_0, D'_0\}$. Finally, this probability can be lower bounded by

$$1 - K_1 \exp(-n\bar{c}) - \frac{K_2}{p^{\bar{d}}},$$

where

$$\begin{aligned} \bar{c} &= \min\left\{\frac{1}{128}, c_2, c_4, c_2 \zeta^{-2}, c_4 \zeta^{-2} \max\{D_0, D'_0\}\right\}, \\ \bar{d} &= \min\{d_2, d'_2\}, \\ K_1 &= 2 + c_1 + c_3, \quad K_2 = \frac{d_1}{2^{d_2}} + \frac{d'_1}{2^{d'_2}}. \end{aligned}$$

This concludes the proof of the main theorem. \square

By slightly weakening the sufficient condition $n \geq \mathcal{D}'' k \log(2p)$ in Theorem 1, we arrive at the following corollary that upper bounds the false positive error probability:

Corollary 1 (False Positive Error Probability). *Suppose that assumptions 1 and 2 as well as conditions 1 and 2 in the proof of Theorem 1 hold. Then, for some arbitrary $t_0 > 0$, thresholding the proposed LGC statistic $\mathcal{T}_{y \rightarrow x}$ at a level $t > 0$ for rejecting the null hypothesis results in a false positive error probability of at most $2 \exp\left(-n/8 \left(1 + \gamma t_0 \sqrt{\log(2p)/n}\right)^2\right)$ with $\gamma := (t + 2)/t$, if*

$$n \geq 2 \max\{\tilde{\mathcal{D}}^2 k^2 / t_0^2, 2\tilde{\mathcal{D}} \gamma k\} \log(2p),$$

for some constant $\tilde{\mathcal{D}}$ that is explicitly given in proof.

Proof. First, we note that under Condition 1 and Condition 2 there exist some real numbers $s, t > 0$ such that

$$\left| \ell(\boldsymbol{\theta}_{(1)}^*, \boldsymbol{\theta}_{(2)}^*) - (\boldsymbol{\Sigma}_\epsilon)_{1,1} \right| \leq (\boldsymbol{\Sigma}_\epsilon)_{1,1}/s, \quad (25a)$$

$$\Delta_F \leq (\boldsymbol{\Sigma}_\epsilon)_{1,1}t/s. \quad (25b)$$

This allows us to set a problem independent threshold, since the upper bound on $\mathcal{T}_{y \rightarrow x}$ under the null hypothesis given in (15) simplifies to:

$$\mathcal{T}_{y \rightarrow x} \leq \frac{2t/s}{1 - (1+t)/s}. \quad (26)$$

Now, given any threshold $t > 0$, we can solve for s in terms of t and t as:

$$s = 1 + \frac{2+t}{t}t = 1 + \gamma t. \quad (27)$$

To ensure $\Delta_F \leq (\boldsymbol{\Sigma}_\epsilon)_{1,1}t/s$, we need the following to hold:

$$\frac{(m+1)\alpha(\boldsymbol{\Sigma}_\epsilon)_{1,1}}{42m} \frac{n}{16s^2} \frac{1}{k \log(2p)} - \frac{1}{t} - \gamma \geq 0. \quad (28)$$

On the other hand, using the expression for s from (27) and invoking Lemma 2 (Appendix C) yield the following statement that can be used to bound the false positive error probability:

$$\mathbb{P} \left[\left| \ell(\boldsymbol{\theta}_{(1)}^*, \boldsymbol{\theta}_{(2)}^*) - (\boldsymbol{\Sigma}_\epsilon)_{1,1} \right| \geq \frac{(\boldsymbol{\Sigma}_\epsilon)_{1,1}}{s} \right] \leq 2 \exp \left(-\frac{n}{8(1+\gamma t)^2} \right). \quad (29)$$

With a choice of $t = t_0 \sqrt{\log(2p)/n}$ for any $t_0 > 0$, applying Lemma 4 (Appendix C) on (28) then gives the sampling requirement of

$$n \geq \left(\tilde{\mathcal{D}}/t_0 \right)^2 k^2 \log(2p) + 2\tilde{\mathcal{D}}\gamma k \log(2p),$$

and the false positive error probability given in the corollary, where

$$\tilde{\mathcal{D}} = \frac{42m}{(m+1)\alpha(\boldsymbol{\Sigma}_\epsilon)_{1,1}} \frac{16A^2}{1}.$$

This concludes the proof of the corollary.

Note that by further choosing $t_0 \geq \sqrt{\tilde{\mathcal{D}}k/2\gamma}$, one can simplify the sampling requirement and the corresponding upper bound on false positive error probability to $n \geq 2 \left(\tilde{\mathcal{D}}/t_0 \right)^2 k^2 \log(2p)$ and $2 \exp \left(-n/(1+\sqrt{8})^2 \right)$, respectively. The later inequality follows from the fact $n \geq 4\tilde{\mathcal{D}}k\gamma \log(2p)$ which is also guaranteed by choice of t_0 . \square

To discuss the implications of these results, several remarks are in order:

Remark 1. Intuitively, detecting a GC effect arising from a small cross-regression coefficient $\boldsymbol{\theta}_{(2)}^*$ is challenging, and often requires a long observation horizon to be identified. Theorem 1 quantifies this intuition via a lower bound on the norm of the cross-regression coefficients in terms of the spectral properties of the process (via \mathcal{B}), sparsity k , sample size n and model order p . In particular, as $\|\boldsymbol{\theta}_{(2)}^*\|_2 \rightarrow 0$, a scaling of $n = \mathcal{O}(k \log(2p)/\|\boldsymbol{\theta}_{(2)}^*\|_2^2)$ maintains the sensitivity/specificity of $\mathcal{T}_{y \rightarrow x}$ with high probability. The lower bound on $\|\boldsymbol{\theta}_{(2)}^*\|_2$ exhibits the same scaling as that in the thresholding procedure of [41] (i.e., the scaling of the LASSO estimation error), as well as the classical scaling of [15], [16] (up to logarithmic factors), and we thus believe is not significantly improvable.

Remark 2. Unlike the conventional estimation error results of the LASSO that specify a lower bound on the regularization parameter λ_n , Theorem 1 prescribes a fixed choice of λ_n for both the *full* and *reduced* estimation problems in (6). This is due to an interesting phenomenon revealed by our analysis: while conventional analyses of LASSO focus on the estimation performance of a single model and thus provide a lower bound on λ_n , in our framework we have two competing models (i.e., *full* and *reduced*) which need to be distinguishable under the null and alternative hypotheses in order to reliably detect the GC influences. The latter imposes an *upper* bound on λ_n . As such, there is a suitable interval for choosing λ_n that results in both consistent estimation and discrimination of the two models. We have presented our results using a single λ_n in this interval for both models, which is appealing from the user’s perspective in practice, where cross-validation is often used for tuning λ_n . The user can select λ_n via cross-validation in solving the LASSO problem for the full model, and then use the same value of λ_n for the reduced model, thus avoiding extra computational costs of cross-validation.

Remark 3. Corollary 1 bounds the false positive error probability, i.e., Type I error rate, for a simple thresholding scheme for detecting GC influences from $\mathcal{T}_{y \rightarrow x}$, under a slightly weakened sufficient condition on n , i.e., $n = \mathcal{O}(k^2 \log(2p))$ instead of $n = \mathcal{O}(k \log(2p))$. This non-asymptotic result provides a principled guideline for choosing a threshold that controls the false positive error rate. As such, this result extends the conventional statistical testing framework based on the asymptotics of log-likelihood ratio statistic using OLS to the non-asymptotic setting using the LASSO. This result can further be utilized in the assignment of p -values (i.e., the false positive error probability when the observed LGC statistic is used as the threshold), as is commonly done in the conventional OLS-based setting based on the asymptotic χ^2 distribution under the null hypothesis. Another advantage of our non-asymptotic result is the involvement of some free variables (e.g., t_0), which can be arbitrarily chosen to sharpen the tests (See, for example, Section IV-B).

Remark 4. We have presented our results for a BVAR model in order to parallel the classical GC analysis. Our results can be extended to the general MVAR setting by using the *conditional* notion of Geweke [9] in a natural fashion, given that Condition 1 and Condition 2 readily generalize to this setting. To elaborate on this point, consider a case where the BVAR(p) model in (1) is augmented by $(d-2)$ other time series to result in a general d -dimensional MVAR(p) setting. Following the formulation of Section II-C, the conditional LGC statistic can be defined as:

$$\mathcal{T}_{y \rightarrow x} := \frac{\ell(\widehat{\boldsymbol{\theta}}_{(1)}, \mathbf{0}, \widehat{\boldsymbol{\theta}}_{(3)}, \dots, \widehat{\boldsymbol{\theta}}_{(d)})}{\ell(\widehat{\boldsymbol{\theta}}_{(1)}, \widehat{\boldsymbol{\theta}}_{(2)}, \widehat{\boldsymbol{\theta}}_{(3)}, \dots, \widehat{\boldsymbol{\theta}}_{(d)})} - 1, \quad (30)$$

where $\widehat{\boldsymbol{\theta}}_{(i)}$ and $\widehat{\boldsymbol{\theta}}_{(i)}$ denote the MVAR parameters from the i^{th} process to the first time series, under the *reduced* and *full* models, respectively. Then, using a similar procedure as in the proof of Theorem 1 and Corollary 1, the results can be extended to this setting, by replacing the various occurrences of $2p$ by dp and by adopting slightly different constants.

Remark 5. The constants in the proof of Theorem 1 and Corollary 1 solely depend on the joint spectrum of processes x_t, y_t as well as some absolute constants. As an illustrative example, by assuming $\boldsymbol{\Sigma}_\epsilon = 0.01\mathbf{I}$, $\mu_{\max}(\mathbf{A}) = 0.9$, $\mu_{\min}(\mathbf{A}) = \mu_{\min}(\check{\mathbf{A}}) = 0.01$, $\widetilde{\Lambda}_{\min} = 0.7$, $\|\mathbf{C}_{11}^{-1}\mathbf{C}_{12}\|_2 = 0.5$, $\|[\mathbf{C}_{11}^{-1}\mathbf{C}_{12}; \mathbf{I}]\boldsymbol{\theta}_{(2)}^*\|_2 = 1.5$, $m = 8$, $d_0 = 5.2 \times 10^{-4}$,

$d'_0 = 4.2 \times 10^{-4}$, $D_0 = 100$, $C_0 = 10^{-6}$, and $c = 0.02$, the key constants in Theorem 1 take the following numerical values: $\mathcal{A} = 10^{-3}$, $\mathcal{B} = 5.136$, $\mathcal{C}' = 7.41 \times 10^{-4}$, $\mathcal{D} = 24.38$, $K_1 = 6$, $K_2 = 6$, $\bar{c} = 2.06 \times 10^{-4}$ and $d = 1$. These translate to $\lambda_n = 10^{-3} \sqrt{\log(2p)/n}$, a requirement of $n > \max\{100, 24.38k\} \log(2p)$, local alternative hypotheses satisfying $\|\theta_{(2)}^*\|_2^2 > 5.136k \log(2p)/n$, and failure probability $< 6 \exp(-2.06 \times 10^{-6}n) + 6/p$. Similarly, for Corollary 1, we get $\tilde{\mathcal{D}} = 10.67$, translating to a sample size requirement of $n > 2 \max\{28.46k^2, 396k\} \log(2p)$ (with $t_0 = 2$ and $t = 0.114$). The potentially large numerical values of some of these constants suggest that the non-asymptotic advantage may come with large values of n and p .

IV. APPLICATION TO SIMULATED AND EXPERIMENTALLY-RECORDED DATA

In this section, we examine our theoretical results through application to simulated and real data, and by comparing the performance of classical OLS-based GC and the proposed LGC statistic in detecting GC influences. We use the fast implementation in [64] to solve the LASSO problems. Unless otherwise stated, the regularization parameter λ_n is chosen via five-fold cross-validation performed over the *full* model, with the same λ_n used for the *reduced* model.

A. Simulation Studies

We simulated three time series x_t, y_t, z_t according to the sparse MVAR(11) model:

$$\begin{aligned} x_t &= -0.67x_{t-1} + 0.2x_{t-5} - 0.1x_{t-11} + 0.05z_{t-3} + \nu_{1,t} \\ y_t &= -0.62y_{t-1} + 0.1y_{t-5} - 0.2y_{t-11} - 0.1x_{t-2} - 0.1x_{t-3} \\ &\quad + 0.5x_{t-11} - 0.001z_{t-4} - 0.004z_{t-5} + \sqrt{0.6}\nu_{2,t} \\ z_t &= -0.9025z_{t-2} + \nu_{3,t} \end{aligned}$$

where $\nu_{i,t} \sim \mathcal{N}(0, 1)$, i.i.d. for $i = 1, 2, 3$. In this model, x_t has a direct causal influence on y_t , but there is no causal influence from y_t to x_t . The *latent* process z_t , however, influences both x_t and y_t (Fig. 1(a)). As such, the correlated process noise components ϵ_t and ϵ'_t in (1) are modeled as $0.05z_{t-3} + \nu_{1,t}$ and $-0.001z_{t-4} - 0.004z_{t-5} + \sqrt{0.6}\nu_{2,t}$,

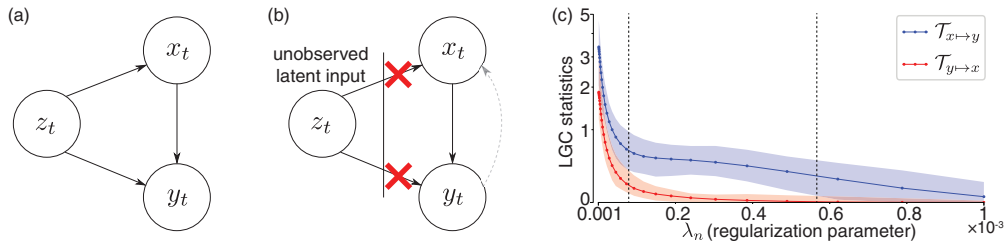


Fig. 1: Simulation Results. (a) Ground truth causality pattern. (b) Estimation setup, in which z_t is latent and thus introduces a spurious causal link (dashed gray arrow) from y_t to x_t . (c) Effect of λ_n on the LGC statistics for $n = 250, p = 100$. The LGC statistics $\mathcal{T}_{y \rightarrow x}$ (red) and $\mathcal{T}_{x \rightarrow y}$ (blue) are separable for a suitable range of λ_n , marked by the dashed vertical lines (colored hulls show the range of LGC over 30 realizations).

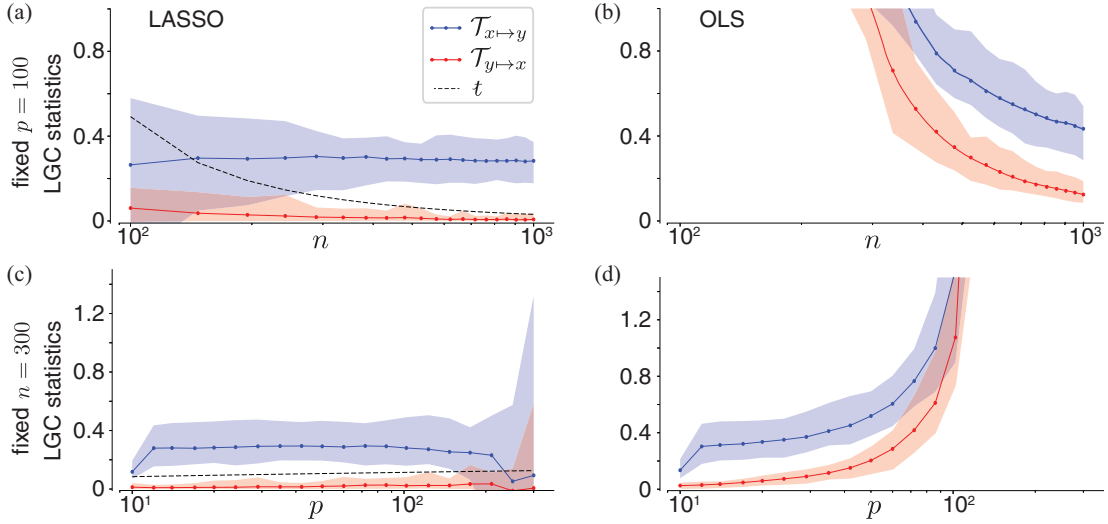


Fig. 2: Simulation Results (continued). LASSO-based (left) and OLS-based ($\lambda_n = 0$, right) LGC statistics $\mathcal{T}_{y \rightarrow x}$ (red) and $\mathcal{T}_{x \rightarrow y}$ (blue) obtained by varying n for fixed $p = 100$ (top panels (a) and (b)) and varying the model order p for fixed $n = 300$ (bottom panels (c) and (d)). The dashed lines in panels (a) and (c) show the threshold t at a false positive error level of 0.01 (colored hulls show the range LGC over 30 realizations).

respectively. As shown in Fig. 1(b), removing z_t from the analysis indeed induces a false (i.e., indirect) causal influence from y_t to x_t . We performed two sets of numerical experiments to evaluate the effects of λ_n , n , and p on the identification of GC influences between x_t and y_t based on $\mathcal{T}_{y \rightarrow x}$ and $\mathcal{T}_{x \rightarrow y}$:

1) *Evaluating the Effect of λ_n* : Fig. 1(c) shows the LGC statistics $\mathcal{T}_{y \rightarrow x}$ (red) and $\mathcal{T}_{x \rightarrow y}$ (blue) for $n = 250$ and $p = 100$, obtained by varying λ_n in the interval $[10^{-6}, 10^{-3}]$ uniformly in the log-scale. The dotted lines and colored hulls represent the average and range of the values, respectively, over 30 realizations. As discussed in *Remark 2*, there is an evident range of λ_n that provides a meaningful separation between $\mathcal{T}_{y \rightarrow x}$ and $\mathcal{T}_{x \rightarrow y}$, which is marked by the dashed vertical lines in Fig. 1(c).

2) *Evaluating the Effect of the Sample Size n* : We fixed a model order of $p = 100$ and varied n uniformly in the interval $[100, 1000]$. Fig. 2(a) and (b) show the resulting LGC statistics $\mathcal{T}_{y \rightarrow x}$ and $\mathcal{T}_{x \rightarrow y}$ corresponding to the LASSO and OLS ($\lambda_n = 0$), respectively. In Fig. 2(a), we also plotted the threshold t corresponding to a false positive probability of 0.01, according to Corollary 1 (dashed line). As n grows larger, the ranges of the two LGC statistics are saliently separated. The proposed thresholding rule of Corollary 1 is also able to correctly identify the true GC effects for $n \geq 250$.

The OLS results shown in Fig. 2(b), however, require much larger values of n to be stable, whereas the LGC statistic provided by the LASSO (Fig. 2(a)) are stable even for $n < 2p$. In addition, OLS requires $n \geq 400$ for the ranges of the GC measures to be distinguishable.

3) *Evaluating the Effect of the Model Order p* : Finally, we fixed $n = 300$ and varied p in the interval $[10, 300]$ uniformly in the log-scale. Fig. 2(c) and (d) show the corresponding GC measures for the LASSO and OLS,

respectively, along with the threshold t corresponding to a false positive probability of 0.01. For $p \ll n$, the LASSO and OLS exhibit similar performance. But, the OLS-based GC measures become unstable for $p \approx n$, whereas those of the LASSO remain stable throughout. The LGC statistics also remain saliently separable over a wider range of p for the LASSO, as compared to their OLS counterparts.

B. Application to Experimentally-Recorded Neural Data from General Anesthesia

Finally, we present an application to simultaneous local field potentials (LFPs) and an ensemble of single-unit recordings from the temporal cortex in a human subject under Propofol-induced general anesthesia (Data from [65]). The LFP signal is the electrical field potential measured at the cortical surface and represents mesoscale dynamics of brain activity with both cortical and subcortical (e.g., thalamic) origins. Single-unit spike recordings, on the other hand, represent the neuronal scale cortical dynamics.

Brain states under anesthesia and sleep are associated with the emergence of periodic and profound suppression of neuronal spiking activity that is strongly phase-locked to the peaks of the LFP slow oscillations [65]–[68]. Specifically, by comparing the average LFP signals triggered at the trough of the slow oscillations under no-spike and many-spike conditions, [66] argues that neuronal spiking activity may have a causal role in high-amplitude peaks of the slow oscillations manifested in the LFP. Here, we examine the role of neuronal spiking activity in mediating the LFP slow oscillations by assessing the GC influences between them.

We use a time duration of 51.2s during anesthesia, corresponding to $n = 1280$ samples (sampling frequency of 25 Hz). The ensemble spiking activity is represented by its peristimulus time histogram (PSTH) (i.e., ensemble average over 23 units). Fig. 3(a) shows the LFP (green) and PSTH (orange) signals used in the analysis. We use

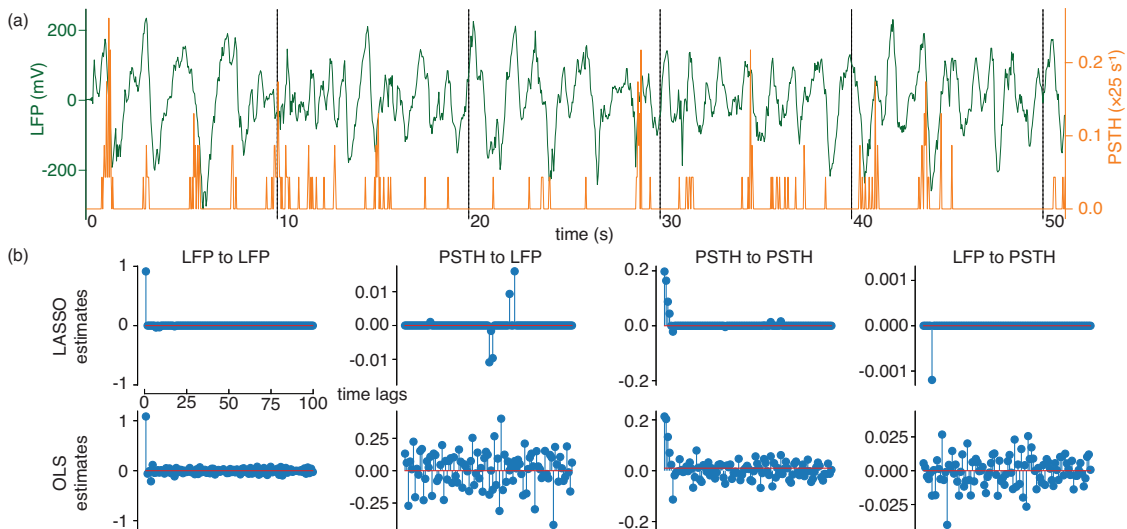


Fig. 3: Analysis of neural data from general anesthesia. (a) LFP (green) and PSTH (orange) traces for a time window of duration 51.2s. (b) BVAR parameter estimates corresponding to the *full* models for LASSO (top) and OLS (bottom).

TABLE I: Obtained LGC Statistics and p -values

	LASSO	OLS
$\mathcal{T}_{\text{LFP} \rightarrow \text{PSTH}}$	0.0055 (0.1079)	0.1001 (0.1832)
$\mathcal{T}_{\text{PSTH} \rightarrow \text{LFP}}$	0.0096 (0.0015)	0.1046 (0.1135)

a model order of $p = 100$, corresponding to a history length of 4 s, to ensure that slow oscillations (~ 0.25 Hz to 0.5 Hz) can be captured by the BVAR model.

Fig. 3(b) shows the estimated BVAR coefficients by the LASSO (top) and OLS (bottom). A visual comparison of the two sets of coefficients suggests that OLS has likely over-fitted the data. The corresponding LGC statistics $\mathcal{T}_{\text{LFP} \rightarrow \text{PSTH}}$ and $\mathcal{T}_{\text{PSTH} \rightarrow \text{LFP}}$ for both methods are reported in Table I. The numbers in parentheses show the p -values, i.e., the false positive error probability, when the observed GC statistics are used as thresholds. For the LGC statistics, the p -values are computed via Corollary 1 (with an arbitrary choice of $t_0 = 0.25$), while in the conventional OLS setting we used the χ^2 distribution against the threshold $\mathcal{F}_{x \rightarrow y} = \log(1 + \mathcal{T}_{x \rightarrow y})$.

For a false positive error probability of 0.01, Corollary 1 clearly detects the GC effect $\text{PSTH} \mapsto \text{LFP}$ (boldface number) as significant, and discards the GC effect $\text{LFP} \mapsto \text{PSTH}$. The conventional χ^2 test applied to the classical GC statistics $\mathcal{F}_{\text{LFP} \rightarrow \text{PSTH}}$ and $\mathcal{F}_{\text{PSTH} \rightarrow \text{LFP}}$, however, fails to detect any GC influence, even at a significance level as high as 0.05. The outcome of the LASSO-based LGC analysis is therefore consistent with the aforementioned hypothesis in [66] on the causal role of spiking activity in mediating the LFP dynamics.

V. CONCLUDING REMARKS

In this work, we proposed a GC statistic based on the LASSO parameter estimates, namely the LGC statistic, in order to identify GC influences in a canonical sparse BVAR model with correlated process noise. By analyzing the non-asymptotic properties of LGC statistic, we established that the well-known sufficient conditions for the consistency of LASSO also suffice for accurate identification of GC influences. By slightly weakening these conditions, we also analyzed the false positive error performance of a simple thresholding rule for detecting GC influences. We validated our theoretical claims through application to simulated and experimentally-recorded neural data from general anesthesia. In particular, we showed that the proposed LGC statistic is able to identify a GC effect from spiking activity to LFP slow oscillations under anesthesia, whereas the conventional OLS-based GC analysis does not detect this effect. Our contribution compared to existing literature is to provide a simple statistic inspired by the classical log-likelihood ratio statistic used for GC analysis, which can be directly computed from the LASSO estimates without the need to resort to de-biasing procedures or asymptotic results for testing. Future work includes extending our results to autoregressive generalized linear models with time-varying parameters.

APPENDIX A

PREDICTION ERROR ANALYSIS OF THE FULL AND REDUCED MODELS

In this section, we establish the deviation bounds of (9) and (10) under Conditions 1 and 2. Note that both the *full* and *reduced* models share the same RE condition (Condition 1), since the *reduced* model is nested within the *full* model. However, the deviation conditions required by Condition 2 are different for the two models. For the *full* model, we require:

$$\left\| \frac{1}{n} \mathbf{X}^\top (\mathbf{x} - \mathbf{X}\boldsymbol{\theta}^*) \right\|_\infty \leq \mathbb{Q}(\boldsymbol{\theta}^*, \boldsymbol{\Sigma}_\epsilon) \sqrt{\frac{\log 2p}{n}}, \quad (31)$$

for some deterministic function $\mathbb{Q}(\boldsymbol{\theta}^*, \boldsymbol{\Sigma}_\epsilon)$. In the *reduced* model, however, we require

$$\left\| \frac{1}{n} \mathbf{X}_{(1)}^\top (\mathbf{x} - \mathbf{X}_{(1)} \tilde{\boldsymbol{\theta}}_{(1)}^*) \right\|_\infty \leq \mathbb{Q}'(\boldsymbol{\theta}^*, \boldsymbol{\Sigma}_\epsilon) \sqrt{\frac{\log 2p}{n}} \quad (32)$$

for another deterministic function $\mathbb{Q}'(\boldsymbol{\theta}^*, \boldsymbol{\Sigma}_\epsilon)$. These conditions guarantee consistent and stable recovery of the autoregressive parameters in the LASSO problems of (6), and hence lead to suitable deviation results for both the *full* and *reduced* models.

Proposition 1 (Deviation Result for the *Full* Model). *Suppose $\widehat{\boldsymbol{\Sigma}} \sim RE(\alpha, \tau)$, with τ satisfying $32k\tau/\alpha = (m-1)/m$ for some $m > 1$ and (\mathbf{X}, \mathbf{x}) satisfying the deviation bound (31). Then for any $\lambda_n \geq 4\mathbb{Q}(\boldsymbol{\theta}^*, \boldsymbol{\Sigma}_\epsilon) \sqrt{\log(2p)/n}$, the solution to the full model in (6) satisfies:*

$$\left| \ell(\widehat{\boldsymbol{\theta}}_{(1)}, \widehat{\boldsymbol{\theta}}_{(2)}) - \ell(\boldsymbol{\theta}_{(1)}^*, \boldsymbol{\theta}_{(2)}^*) \right| \leq \frac{24}{m+1} \frac{k\lambda_n^2}{\alpha/m} =: \Delta_F. \quad (33)$$

Proof. For the *full* model, we have:

$$\ell(\widehat{\boldsymbol{\theta}}_{(1)}, \widehat{\boldsymbol{\theta}}_{(2)}) - \ell(\boldsymbol{\theta}_{(1)}^*, \boldsymbol{\theta}_{(2)}^*) = \frac{1}{n} (\widehat{\boldsymbol{\theta}} - \boldsymbol{\theta}^*)^\top \mathbf{X}^\top \mathbf{X} (\widehat{\boldsymbol{\theta}} - \boldsymbol{\theta}^*) + \frac{2}{n} (\widehat{\boldsymbol{\theta}} - \boldsymbol{\theta}^*)^\top \mathbf{X}^\top (\mathbf{x} - \mathbf{X}\boldsymbol{\theta}^*). \quad (34)$$

To obtain bounds on the left hand side of (34), we bound the terms on the right hand side individually. The bound on the first term follows from (39) on the consistency of the LASSO under the RE and deviation bound assumptions (See Proposition 3),

$$\frac{1}{n} (\widehat{\boldsymbol{\theta}} - \boldsymbol{\theta}^*)^\top \mathbf{X}^\top \mathbf{X} (\widehat{\boldsymbol{\theta}} - \boldsymbol{\theta}^*) \leq \frac{18m}{m+1} \frac{k\lambda_n^2}{\alpha},$$

while the second terms can be bounded using (38) as

$$\left| \frac{1}{n} (\widehat{\boldsymbol{\theta}} - \boldsymbol{\theta}^*)^\top \mathbf{X}^\top (\mathbf{x} - \mathbf{X}\boldsymbol{\theta}^*) \right| \leq \left\| \widehat{\boldsymbol{\theta}} - \boldsymbol{\theta}^* \right\|_1 \left\| \frac{1}{n} \mathbf{X}^\top (\mathbf{x} - \mathbf{X}\boldsymbol{\theta}^*) \right\|_\infty \leq \frac{3m}{m+1} \frac{k\lambda_n^2}{\alpha},$$

where we have used the choice of λ_n and (31) to conclude:

$$\left\| \mathbf{X}^\top (\mathbf{x} - \mathbf{X}\boldsymbol{\theta}^*) \right\|_\infty \leq \frac{\lambda_n}{4}.$$

Combining these two bounds via the triangle inequality concludes the proof. \square

Proposition 2 (Deviation Result for the *Reduced* Model). *Suppose $\widehat{\boldsymbol{\Sigma}} \sim RE(\alpha, \tau)$, with τ satisfying $32k\tau/\alpha = (m-1)/m$ for some $m > 1$ and $(\mathbf{X}_{(1)}, \mathbf{x})$ satisfying the deviation bound (32). Let J denote the support of $\boldsymbol{\theta}_{(1)}^*$,*

with its complement denoted by J^c . Then, for any $\lambda_n \geq 4\mathbb{Q}'(\boldsymbol{\theta}^*, \boldsymbol{\Sigma}_\epsilon)\sqrt{\log 2p/n}$, the solution to reduced model in (6) satisfies:

$$\left| \ell\left(\widehat{\boldsymbol{\theta}}_{(1)}, \mathbf{0}\right) - \ell\left(\widetilde{\boldsymbol{\theta}}_{(1)}^*, \mathbf{0}\right) \right| \leq 20 \frac{k\lambda_n^2}{\alpha/m} + \left(8\sqrt{2m} + 18\right) \lambda_n \left\| \widetilde{\boldsymbol{\theta}}_{(1)J^c}^* \right\|_1 =: \Delta_R, \quad (35)$$

Proof. In a similar fashion to Proposition 1, by invoking the consistency results of LASSO for the *reduced* model under the RE and deviation bound assumptions (See Proposition 4) and noting (32) we have:

$$\left| \ell\left(\widehat{\boldsymbol{\theta}}_{(1)}, \mathbf{0}\right) - \ell\left(\widetilde{\boldsymbol{\theta}}_{(1)}^*, \mathbf{0}\right) \right| \leq 12 \frac{k\lambda_n^2}{\alpha/m} + \left(8\left(\sqrt{2m} + 1\right) + 2\right) \lambda_n \left\| \widetilde{\boldsymbol{\theta}}_{(1)J^c}^* \right\|_1 + 16 \sqrt{\frac{\lambda_n^3 k}{\alpha/m}} \sqrt{\left\| \widetilde{\boldsymbol{\theta}}_{(1)J^c}^* \right\|_1}. \quad (36)$$

Simplifying the last term using Arithmetic Mean-Geometric Mean inequality proves the claim. \square

To establish the consistency results used in Proposition 1 and Proposition 2, we first state a result adapted from [26] on the prediction error of LASSO under the *full* model:

Proposition 3 (Prediction Error for the *Full* Model). *Suppose $\widehat{\boldsymbol{\Sigma}} \sim RE(\alpha, \tau)$, with τ satisfying $32k\tau/\alpha = (m-1)/m$ for some $m > 1$ and (\mathbf{X}, \mathbf{x}) satisfying the deviation bound (31). Then for any $\lambda_n \geq 4\mathbb{Q}'(\boldsymbol{\theta}^*, \boldsymbol{\Sigma}_\epsilon)\sqrt{\frac{\log(2p)}{n}}$, the solution to the full model in (6) satisfies:*

$$\left\| \widehat{\boldsymbol{\theta}} - \boldsymbol{\theta}^* \right\|_2 \leq \frac{3m}{m+1} \frac{\sqrt{k}\lambda_n}{\alpha}, \quad (37)$$

$$\left\| \widehat{\boldsymbol{\theta}} - \boldsymbol{\theta}^* \right\|_1 \leq \frac{12m}{m+1} \frac{k\lambda_n}{\alpha}, \quad (38)$$

$$\left(\widehat{\boldsymbol{\theta}} - \boldsymbol{\theta}^*\right)^\top \widehat{\boldsymbol{\Sigma}} \left(\widehat{\boldsymbol{\theta}} - \boldsymbol{\theta}^*\right) \leq \frac{18m}{m+1} \frac{k\lambda_n^2}{\alpha}. \quad (39)$$

Proof. The proof closely follows that of [26, Proposition 4.1], and is thus omitted for brevity. \square

In what follows, we show that the particular choice of τ satisfying $32k\tau/\alpha = (m-1)/m$ for some $m > 1$ will simplify the prediction error analysis of the *reduced* model. As for the *reduced* model, the main technical difficulty in establishing prediction error bounds stems from the fact that $\widetilde{\boldsymbol{\theta}}_{(1)}^*$ is no longer k -sparse. We address this issue in the following proposition:

Proposition 4 (Prediction Error for the *Reduced* Model). *Suppose $\widehat{\boldsymbol{\Sigma}} \sim RE(\alpha, \tau)$, with τ satisfying the relation in Proposition 3 and $(\mathbf{X}_{(1)}, \mathbf{x})$ satisfying the deviation bound (32). Let J denote the support of $\boldsymbol{\theta}_{(1)}^*$, with its complement denoted by J^c . Then, for any $\lambda_n \geq 4\mathbb{Q}'(\boldsymbol{\theta}^*, \boldsymbol{\Sigma}_\epsilon)\sqrt{\log 2p/n}$, the solution to reduced model in (6) satisfies the following inequalities:*

$$\left\| \widehat{\boldsymbol{\theta}}_{(1)} - \widetilde{\boldsymbol{\theta}}_{(1)}^* \right\|_2 \leq \frac{3}{2} \frac{\lambda_n \sqrt{k}}{\alpha/m} + \sqrt{\frac{2m}{k}} \left\| \widetilde{\boldsymbol{\theta}}_{(1)J^c}^* \right\|_1 + \sqrt{\frac{4\lambda_n}{\alpha/m}} \left\| \widetilde{\boldsymbol{\theta}}_{(1)J^c}^* \right\|_1, \quad (40)$$

$$\left\| \widehat{\boldsymbol{\theta}}_{(1)} - \widetilde{\boldsymbol{\theta}}_{(1)}^* \right\|_1 \leq 6 \frac{\lambda_n k}{\alpha/m} + 4(\sqrt{2m} + 1) \left\| \widetilde{\boldsymbol{\theta}}_{(1)J^c}^* \right\|_1 + 8 \sqrt{\frac{\lambda_n k}{\alpha/m}} \sqrt{\left\| \widetilde{\boldsymbol{\theta}}_{(1)J^c}^* \right\|_1}, \quad (41)$$

$$\frac{1}{n} \left(\widehat{\boldsymbol{\theta}}_{(1)} - \widetilde{\boldsymbol{\theta}}_{(1)}^*\right)^\top \mathbf{X}_{(1)}^\top \mathbf{X}_{(1)} \left(\widehat{\boldsymbol{\theta}}_{(1)} - \widetilde{\boldsymbol{\theta}}_{(1)}^*\right) \leq 9 \frac{\lambda_n^2 k}{\alpha/m} \left(6\left(\sqrt{2m} + 1\right) + 2\right) \lambda_n \left\| \widetilde{\boldsymbol{\theta}}_{(1)J^c}^* \right\|_1 + 12 \sqrt{\frac{\lambda_n^3 k}{\alpha/m}} \sqrt{\left\| \widetilde{\boldsymbol{\theta}}_{(1)J^c}^* \right\|_1}. \quad (42)$$

Proof. Recall that $\tilde{\boldsymbol{\theta}}_{(1)}^* := \boldsymbol{\theta}_{(1)}^* + \mathbf{C}_{11}^{-1} \mathbf{C}_{21} \boldsymbol{\theta}_{(2)}^*$. Let us define

$$F(\boldsymbol{\theta}_{(1)}) := \frac{1}{n} \|\mathbf{x} - \mathbf{X}_{(1)} \boldsymbol{\theta}_{(1)}\|_2^2 + \lambda_n \|\boldsymbol{\theta}_{(1)}\|_1.$$

and consider the quantity, $\Delta F(\hat{\boldsymbol{\theta}}_{(1)}) := F(\hat{\boldsymbol{\theta}}_{(1)}) - F(\tilde{\boldsymbol{\theta}}_{(1)}^*)$. Also, let $\mathbf{v} := \boldsymbol{\theta}_{(1)}^* - \hat{\boldsymbol{\theta}}_{(1)}$ and $\tilde{\mathbf{v}} := \mathbf{v} + \mathbf{C}_{11}^{-1} \mathbf{C}_{12} \boldsymbol{\theta}_{(2)}^*$.

Then, $\Delta F(\hat{\boldsymbol{\theta}}_{(1)})$ can be simplified as:

$$\begin{aligned} \Delta F(\hat{\boldsymbol{\theta}}_{(1)}) &= F(\hat{\boldsymbol{\theta}}_{(1)}) - F(\tilde{\boldsymbol{\theta}}_{(1)}^*) \\ &= \frac{1}{n} \tilde{\mathbf{v}}^\top \mathbf{X}_{(1)}^\top \mathbf{X}_{(1)} \tilde{\mathbf{v}} + \frac{2}{n} \mathbf{X}_{(1)}^\top (\mathbf{x} - \mathbf{X}_{(1)} \tilde{\boldsymbol{\theta}}_{(1)}^*) + \lambda_n \left(\|\hat{\boldsymbol{\theta}}_{(1)}\|_1 - \|\tilde{\boldsymbol{\theta}}_{(1)}^*\|_1 \right). \end{aligned}$$

Using the fact that

$$\left\| \frac{2}{n} \mathbf{X}_{(1)}^\top (\mathbf{x} - \mathbf{X}_{(1)} \tilde{\boldsymbol{\theta}}_{(1)}^*) \right\|_\infty \geq \frac{\lambda_n}{2},$$

we get:

$$\Delta F(\hat{\boldsymbol{\theta}}_{(1)}) \geq \frac{1}{n} \tilde{\mathbf{v}}^\top \mathbf{X}_{(1)}^\top \mathbf{X}_{(1)} \tilde{\mathbf{v}} - \frac{\lambda_n}{2} (\|\tilde{\mathbf{v}}_J\|_1 + \|\tilde{\mathbf{v}}_{J^c}\|_1) + \lambda_n \left(\|\tilde{\mathbf{v}}_{J^c}\|_1 - \|\tilde{\mathbf{v}}_J\|_1 - 2 \|\tilde{\boldsymbol{\theta}}_{(1)J^c}^*\|_1 \right),$$

where we split the error $\tilde{\mathbf{v}}$ into components within J and components within J^c . Now, since $\tilde{\mathbf{v}}^\top \mathbf{X}_{(1)}^\top \mathbf{X}_{(1)} \tilde{\mathbf{v}}$ is non-negative, we arrive at:

$$\begin{aligned} 0 &\geq -\frac{\lambda_n}{2} (\|\tilde{\mathbf{v}}_J\|_1 + \|\tilde{\mathbf{v}}_{J^c}\|_1) + \lambda_n \left(\|\tilde{\mathbf{v}}_{J^c}\|_1 - \|\tilde{\mathbf{v}}_J\|_1 - 2 \|\tilde{\boldsymbol{\theta}}_{(1)J^c}^*\|_1 \right) \\ &= -\frac{\lambda_n}{2} \left(3 \|\tilde{\mathbf{v}}_J\|_1 - \|\tilde{\mathbf{v}}_{J^c}\|_1 + 4 \|\tilde{\boldsymbol{\theta}}_{(1)J^c}^*\|_1 \right). \end{aligned} \quad (43)$$

The rest of the treatment follows the derivation of weakly sparse or compressible models (See, for example, the derivation of the main theorem in [32]). Using the inequality (43), we can write:

$$\|\tilde{\mathbf{v}}\|_1 = \|\tilde{\mathbf{v}}_J\|_1 + \|\tilde{\mathbf{v}}_{J^c}\|_1 \leq 4 \|\tilde{\mathbf{v}}_J\|_1 + 4 \|\tilde{\boldsymbol{\theta}}_{(1)J^c}^*\|_1 \leq 4\sqrt{k} \|\tilde{\mathbf{v}}_J\|_2 + 4 \|\tilde{\boldsymbol{\theta}}_{(1)J^c}^*\|_1, \quad (44)$$

where the last inequality follows from the fact $|J| \leq k$. This inequality together with the RE condition and τ satisfying the relation in Proposition 3, allows to write:

$$\begin{aligned} \frac{1}{n} \tilde{\mathbf{v}}^\top \mathbf{X}_{(1)}^\top \mathbf{X}_{(1)} \tilde{\mathbf{v}} &\geq \alpha \|\tilde{\mathbf{v}}\|_2^2 - \alpha \frac{m-1}{m} \|\tilde{\mathbf{v}}\|_2^2 - \frac{\alpha}{m} \frac{m-1}{k} \|\tilde{\boldsymbol{\theta}}_{(1)J^c}^*\|_1^2 \\ &\geq \frac{\alpha}{m} \|\tilde{\mathbf{v}}\|_2^2 - \frac{\alpha}{m} \frac{m-1}{k} \|\tilde{\boldsymbol{\theta}}_{(1)J^c}^*\|_1^2, \end{aligned} \quad (45)$$

using the inequality $\sqrt{2(a^2 + b^2)} \geq (a + b)$.

Combining (43) and (45), we then finally arrive at:

$$\begin{aligned} \Delta F(\hat{\boldsymbol{\theta}}_{(1)}) &\geq \frac{\alpha}{m} \|\tilde{\mathbf{v}}\|_2^2 - \frac{\alpha}{m} \frac{m-1}{k} \|\tilde{\boldsymbol{\theta}}_{(1)J^c}^*\|_1^2 - \frac{\lambda_n}{2} \left(3 \|\tilde{\mathbf{v}}_J\|_1 - \|\tilde{\mathbf{v}}_{J^c}\|_1 + 4 \|\tilde{\boldsymbol{\theta}}_{(1)J^c}^*\|_1 \right) \\ &\geq \frac{\alpha}{m} \|\tilde{\mathbf{v}}\|_2^2 - \frac{\alpha}{m} \frac{m-1}{k} \|\tilde{\boldsymbol{\theta}}_{(1)J^c}^*\|_1^2 - \frac{\lambda_n}{2} \left(3\sqrt{k} \|\tilde{\mathbf{v}}\|_2 + 4 \|\tilde{\boldsymbol{\theta}}_{(1)J^c}^*\|_1 \right), \end{aligned} \quad (46)$$

where the last step follows from the inequalities $\|\tilde{\mathbf{v}}_J\|_1 \leq \sqrt{k} \|\tilde{\mathbf{v}}_J\|_2 \leq \sqrt{k} \|\tilde{\mathbf{v}}\|_2$ and $\|\tilde{\mathbf{v}}_{J^c}\|_1 \geq 0$.

An application of Lemma 4 establishes that the right hand side of the inequality (46) will be positive if:

$$\|\tilde{\mathbf{v}}\|_2^2 \geq \frac{9}{4} \frac{\lambda_n^2}{\alpha^2/m^2} k + \frac{\lambda_n}{\alpha/m} \left(\frac{2}{\lambda_n} \frac{\alpha}{m} \frac{m-1}{k} \|\tilde{\boldsymbol{\theta}}_{(1)J^c}^*\|_1^2 + 4 \|\tilde{\boldsymbol{\theta}}_{(1)J^c}^*\|_1 \right). \quad (47)$$

From the latter inequality, the first claim of the proposition follows using the fact that $\|\mathbf{a}\|_1 \geq \|\mathbf{a}\|_2$; the second claim follows from the first claim together with (44); the last claim follows from the fact that:

$$\frac{1}{n} \tilde{\mathbf{v}}^\top \mathbf{X}_{(1)}^\top \mathbf{X}_{(1)} \tilde{\mathbf{v}} \leq \frac{\lambda_n}{2} \left(3 \|\tilde{\mathbf{v}}_J\|_1 - \|\tilde{\mathbf{v}}_{J^c}\|_1 + 4 \left\| \tilde{\boldsymbol{\theta}}_{(1), J^c}^* \right\|_1 \right), \quad (48)$$

which concludes the proof of the proposition. \square

APPENDIX B

VERIFICATION OF CONDITIONS 1 AND 2

Having established Propositions 1 and 2, it only remains to show that Condition 1 and Condition 2 hold with high probability, under both the *full* and *reduced* models.

The following proposition establishes that the RE condition (Condition 1) holds with high probability:

Proposition 5 (Verifying RE for $\hat{\boldsymbol{\Sigma}} = \mathbf{X}^\top \mathbf{X}/n$). *Let*

$$\zeta := 54 \frac{\Lambda_{\max}(\boldsymbol{\Sigma}_\epsilon)/\mu_{\min}(\check{\mathbf{A}})}{\Lambda_{\min}(\boldsymbol{\Sigma}_\epsilon)/\mu_{\max}(\mathbf{A})}, \quad \alpha := \frac{\Lambda_{\min}(\boldsymbol{\Sigma}_\epsilon)}{2\mu_{\max}(\mathbf{A})}, \quad \tau := \frac{4\alpha \max\{\zeta^2, 1\} \log 2p}{c n}.$$

Then, for $n \geq C_0 \max\{\zeta^2, 1\} k \log 2p$, there exist constants c_1, c_2 such that

$$\mathbb{P} \left[\hat{\boldsymbol{\Sigma}} \sim RE(\alpha, \tau) \right] \geq 1 - c_1 \exp(-c_2 n \min\{\zeta^{-2}, 1\}). \quad (49)$$

Proof. The proof closely follows that of [26, proof of Proposition 4.2], and is thus omitted for brevity. \square

Remark 6. In order for τ to satisfy $32k\tau/\alpha = (m-1)/m$ for some $m > 1$, we precisely need $n \geq (128/c)(m/(m-1)) \max\{\zeta^2, 1\} k \log(2p)$.

Finally, the following two propositions establish that the deviation conditions (Condition 2) hold with high probability.

Proposition 6 (Deviation Condition for the *full* Model). *For $n \geq D_0 \log(2p)$, there exist constants d_0, d_1 and $d_2 > 0$ such that*

$$\mathbb{P} \left[\left\| \frac{1}{n} \mathbf{X}^\top (\mathbf{x} - \mathbf{X}\boldsymbol{\theta}^*) \right\|_\infty \geq \mathbb{Q}(\boldsymbol{\theta}^*, \boldsymbol{\Sigma}_\epsilon) \sqrt{\frac{\log 2p}{n}} \right] \leq \frac{d_1}{(2p)^{d_2}}, \quad (50)$$

where

$$\mathbb{Q}(\boldsymbol{\theta}^*, \boldsymbol{\Sigma}_\epsilon) := d_0 \Lambda_{\max}(\boldsymbol{\Sigma}_\epsilon) \left(1 + \frac{1 + \mu_{\max}(\mathbf{A})}{\mu_{\min}(\mathbf{A})} \right).$$

Proof. The proof follows that of [26, Proposition 4.3], and is thus omitted for brevity. \square

Proposition 7 (Deviation Condition for the *Reduced* Model). *For $n \geq D'_0 \log(2p)$, there exist constants d'_0, d'_1 , and $d'_2 > 0$ such that*

$$\mathbb{P} \left[\left\| \frac{1}{n} \mathbf{X}_{(1)}^\top (\mathbf{x} - \mathbf{X}_{(1)} \tilde{\boldsymbol{\theta}}_{(1)}^*) \right\|_\infty \geq \mathbb{Q}'(\boldsymbol{\theta}^*, \boldsymbol{\Sigma}_\epsilon) \sqrt{\frac{\log 2p}{n}} \right] \leq \frac{d'_1}{(2p)^{d'_2}}, \quad (51)$$

where $\mathbb{Q}'(\boldsymbol{\theta}^*, \boldsymbol{\Sigma}_\epsilon)$ is defined as:

$$\mathbb{Q}'(\boldsymbol{\theta}^*, \boldsymbol{\Sigma}_\epsilon) := d'_0 \Lambda_{\max}(\boldsymbol{\Sigma}_\epsilon) \left(1 + \frac{1 + \mu_{\max}(\mathbf{A})}{\mu_{\min}(\mathbf{A})} + \frac{3 \left\| \left[-\mathbf{C}_{11}^{-1} \mathbf{C}_{12} \boldsymbol{\theta}_{(2)}^*; \boldsymbol{\theta}_{(2)}^* \right] \right\|_2}{\mu_{\min}(\check{\mathbf{A}})} \right) \quad (52)$$

Proof. In the *reduced* model, the deviation can be expressed as:

$$\begin{aligned} & \frac{1}{n} \mathbf{X}_{(1)} \left(\mathbf{x} - \mathbf{X}_{(1)} \tilde{\boldsymbol{\theta}}_{(1)}^* - \mathbf{X}_{(2)} \mathbf{0} \right) \\ &= \frac{1}{n} \mathbf{X}_{(1)}^\top \left(-\mathbf{X}_{(1)} \mathbf{C}_{11}^{-1} \mathbf{C}_{12} \boldsymbol{\theta}_{(2)}^* + \mathbf{X}_{(2)} \boldsymbol{\theta}_{(2)}^* + \boldsymbol{\epsilon} \right) \\ &= -\frac{1}{n} \mathbf{X}_{(1)}^\top \mathbf{X}_{(1)} \mathbf{C}_{11}^{-1} \mathbf{C}_{12} \boldsymbol{\theta}_{(2)}^* + \frac{1}{n} \mathbf{X}_{(1)}^\top \mathbf{X}_{(2)} \boldsymbol{\theta}_{(2)}^* + \frac{1}{n} \mathbf{X}_{(1)}^\top \boldsymbol{\epsilon} \end{aligned}$$

The last term can be bounded in a similar fashion as done for the deviation in Proposition 6. The i^{th} component of the first two terms can be expressed as $\mathbf{e}_i^\top \frac{1}{n} \mathbf{X}^\top \mathbf{X} \left[-\mathbf{C}_{11}^{-1} \mathbf{C}_{12} \boldsymbol{\theta}_{(2)}^*; \boldsymbol{\theta}_{(2)}^* \right]$, for $i = 1, 2, \dots, p$ where \mathbf{e}_i 's are the standard unit bases in \mathbb{R}^{2p} . Invoking [26, Proposition 2.4(a)] and noting that $\mathcal{M}(\mathbf{F}) \leq \Lambda_{\max}(\boldsymbol{\Sigma}_\epsilon) / \mu_{\min}(\check{\mathbf{A}})$, we get:

$$\mathbb{P} \left[\left| \mathbf{e}_i^\top \frac{1}{n} \mathbf{X}^\top \mathbf{X} \left[-\mathbf{C}_{11}^{-1} \mathbf{C}_{12} \boldsymbol{\theta}_{(2)}^*; \boldsymbol{\theta}_{(2)}^* \right] \right| \geq 3 \frac{\Lambda_{\max}(\boldsymbol{\Sigma}_\epsilon)}{\mu_{\min}(\check{\mathbf{A}})} \eta \left\| \left[-\mathbf{C}_{11}^{-1} \mathbf{C}_{12} \boldsymbol{\theta}_{(2)}^*; \boldsymbol{\theta}_{(2)}^* \right] \right\|_2 \right] \leq 6 \exp[-cn \min\{\eta, \eta^2\}] \quad (53)$$

Using the union bound, we can then arrive at:

$$\begin{aligned} \mathbb{P} \left[\left| \frac{1}{n} \mathbf{e}_i^\top \left(\mathbf{X}^\top \mathbf{X} \left[-\mathbf{C}_{11}^{-1} \mathbf{C}_{12} \boldsymbol{\theta}_{(2)}^*; \boldsymbol{\theta}_{(2)}^* \right] + \mathbf{X}^\top \boldsymbol{\epsilon} \right) \right| \geq \Lambda_{\max}(\boldsymbol{\Sigma}_\epsilon) \left(1 + \frac{1 + \mu_{\max}(\mathbf{A})}{\mu_{\min}(\mathbf{A})} + \frac{3 \left\| \left[-\mathbf{C}_{11}^{-1} \mathbf{C}_{12} \boldsymbol{\theta}_{(2)}^*; \boldsymbol{\theta}_{(2)}^* \right] \right\|_2}{\mu_{\min}(\check{\mathbf{A}})} \right) \eta \right] \\ \leq 12 \exp[-cn \min\{\eta, \eta^2\}] \end{aligned} \quad (54)$$

Using the latter inequality, the statement of the proposition follows from the same arguments used in the proof of [26, Proposition 4.3]. \square

APPENDIX C

CONCENTRATION INEQUALITIES AND TECHNICAL LEMMAS

Lemma 1. *Given i.i.d. samples from a normal distribution, i.e., $w_t \sim \mathcal{N}(0, \sigma^2)$, the following holds:*

$$\mathbb{P} \left[\left| \frac{1}{n} \sum_{t=1}^n \frac{w_t^2}{\sigma^2} - 1 \right| \geq t \right] \leq 2 \exp \left(-\frac{nt^2}{8} \right) \quad (55)$$

Proof. Define $z_t = w_t/\sigma \sim \mathcal{N}(0, 1)$, then $\sum_{t=1}^n z_t^2 \sim \chi^2(n)$. Clearly, z_t^2 is sub-exponential with parameters (2, 4), so is the sum $\sum_{t=1}^n z_t^2$ with parameters $(2\sqrt{n}, 4)$. The claim of the lemma then follows from standard sub-exponential tail bounds. \square

Lemma 2 (Concentration of the *Full* Model Deviation). *Under the full model, we have:*

$$\mathbb{P} \left[\left| \ell \left(\boldsymbol{\theta}_{(1)}^*, \boldsymbol{\theta}_{(2)}^* \right) - (\boldsymbol{\Sigma}_\epsilon)_{1,1} \right| \geq \Delta_N \right] \leq 2 \exp \left(-\frac{n\Delta_N^2}{8(\boldsymbol{\Sigma}_\epsilon)_{1,1}^2} \right).$$

Proof. Note that $\ell \left(\boldsymbol{\theta}_{(1)}^*, \boldsymbol{\theta}_{(2)}^* \right) = \sum_{t=1}^n \epsilon_t^2/n$. Since $\epsilon_t \sim \mathcal{N}(0, (\boldsymbol{\Sigma}_\epsilon)_{1,1})$, using Lemma 1 we get:

$$\mathbb{P} \left[\left| \frac{1}{n} \sum_{t=1}^n \frac{\epsilon_t^2}{(\boldsymbol{\Sigma}_\epsilon)_{1,1}} - 1 \right| \geq t \right] \leq 2 \exp \left(-\frac{nt^2}{8} \right). \quad (56)$$

By letting $\Delta_N := t(\boldsymbol{\Sigma}_\epsilon)_{1,1}$, the claim of the lemma follows. \square

Lemma 3 (Concentration of the *Reduced Model Deviation*). *Suppose that the deviation conditions (Condition 2) hold. Then, there exist constants c_3 and $c_4 > 0$ such that*

$$\left| \ell(\tilde{\boldsymbol{\theta}}_{(1)}^*, \mathbf{0}) - \ell(\boldsymbol{\theta}_{(1)}^*, \boldsymbol{\theta}_{(2)}^*) - D \right| \leq \Delta_D, \quad (57)$$

with probability at least

$$1 - c_3 \exp\left(-c_4 n \min\left\{\zeta^{-2} \frac{\log 2p}{n}, 1\right\}\right),$$

$$\Delta_D := \mathbb{Q}(\boldsymbol{\theta}^*, \boldsymbol{\Sigma}_\epsilon) \sqrt{\frac{\log 2p}{n}} \left\| \left[-\mathbf{C}_{11}^{-1} \mathbf{C}_{12} \boldsymbol{\theta}_{(2)}^*; \boldsymbol{\theta}_{(2)}^* \right] \right\|_1 + \frac{\alpha}{27} \left\| \left[-\mathbf{C}_{11}^{-1} \mathbf{C}_{12} \boldsymbol{\theta}_{(2)}^*; \boldsymbol{\theta}_{(2)}^* \right] \right\|_2^2,$$

and

$$D := \boldsymbol{\theta}_{(2)}^{*\top} (\mathbf{C}_{22} - \mathbf{C}_{21} \mathbf{C}_{11}^{-1} \mathbf{C}_{12}) \boldsymbol{\theta}_{(2)}^*.$$

with α and $\mathbb{Q}(\boldsymbol{\theta}^*, \boldsymbol{\Sigma}_\epsilon)$ defined in Proposition 5 and Proposition 6, respectively.

Proof. Since $\tilde{\boldsymbol{\theta}}_{(1)}^* = \boldsymbol{\theta}_{(1)}^* + \mathbf{C}_{11}^{-1} \mathbf{C}_{12} \boldsymbol{\theta}_{(2)}^*$, we have:

$$\begin{aligned} \ell(\tilde{\boldsymbol{\theta}}_{(1)}^*, \mathbf{0}) - \ell(\boldsymbol{\theta}_{(1)}^*, \boldsymbol{\theta}_{(2)}^*) &= \frac{1}{n} \left\| \mathbf{x} - \mathbf{X}_{(1)} \tilde{\boldsymbol{\theta}}_{(1)}^* - \mathbf{X}_{(2)} \mathbf{0} \right\|_2^2 - \frac{1}{n} \left\| \mathbf{x} - \mathbf{X} \boldsymbol{\theta}^* \right\|_2^2 \\ &= \frac{1}{n} \left\| -\mathbf{X}_{(1)} \mathbf{C}_{11}^{-1} \mathbf{C}_{12} \boldsymbol{\theta}_{(2)}^* + \mathbf{X}_{(2)} \boldsymbol{\theta}_{(2)}^* + \boldsymbol{\epsilon} \right\|_2^2 - \frac{1}{n} \left\| \boldsymbol{\epsilon} \right\|_2^2 \\ &= \frac{2}{n} \boldsymbol{\epsilon}^\top \mathbf{X} \boldsymbol{\vartheta} + \boldsymbol{\vartheta}^\top \frac{1}{n} \mathbf{X}^\top \mathbf{X} \boldsymbol{\vartheta}, \end{aligned}$$

where $\boldsymbol{\vartheta} := \left[(-\mathbf{C}_{11}^{-1} \mathbf{C}_{12} \boldsymbol{\theta}_{(2)}^*)^\top, \boldsymbol{\theta}_{(2)}^{*\top} \right]^\top$. Using the Condition 2, we get:

$$\begin{aligned} \left| \frac{1}{n} \boldsymbol{\epsilon}^\top \mathbf{X} \boldsymbol{\vartheta} \right| &\leq \left\| \frac{1}{n} \mathbf{X}^\top \boldsymbol{\epsilon} \right\|_\infty \|\boldsymbol{\vartheta}\|_1 \\ &\leq \mathbb{Q}(\boldsymbol{\theta}^*, \boldsymbol{\Sigma}_\epsilon) \sqrt{\frac{\log 2p}{n}} \|\boldsymbol{\vartheta}\|_1 \\ &\leq \mathbb{Q}(\boldsymbol{\theta}^*, \boldsymbol{\Sigma}_\epsilon) \sqrt{\frac{\log 2p}{n}} (\|\mathbf{C}_{11}^{-1} \mathbf{C}_{12}\|_1 + 1) \|\boldsymbol{\theta}_{(2)}^*\|_1. \end{aligned}$$

Furthermore, from [26, Proposition 2.4], for any $\boldsymbol{\vartheta} \in \mathbb{R}^{2p}$ and $\eta \geq 0$, there exists a constant $c > 0$ such that:

$$\mathbb{P} \left[\left| \boldsymbol{\vartheta}^\top \left(\frac{1}{n} \mathbf{X}^\top \mathbf{X} - \mathbf{C} \right) \boldsymbol{\vartheta} \right| \geq \eta \|\boldsymbol{\vartheta}\|^2 \frac{\Lambda_{\max}(\boldsymbol{\Sigma}_\epsilon)}{\mu_{\min}(\tilde{\mathbf{A}})} \right] \leq 2 \exp[-cn \min\{\eta, \eta^2\}].$$

Next, with the choice of $\eta = \zeta^{-1} \sqrt{\log 2p/n}$, the latter concentration inequality establishes that:

$$\left| \boldsymbol{\vartheta}^\top \left(\frac{1}{n} \mathbf{X}^\top \mathbf{X} \right) \boldsymbol{\vartheta} - \boldsymbol{\vartheta}^\top \mathbf{C} \boldsymbol{\vartheta} \right| \leq \frac{\alpha}{27} \sqrt{\frac{\log 2p}{n}} \|\boldsymbol{\vartheta}\|_2^2,$$

with probability at least $1 - 2 \exp(-cn \min\{\zeta^{-2} \log 2p/n, 1\})$. This along with the following observation concludes the proof of the lemma: $\boldsymbol{\vartheta}^\top \mathbf{C} \boldsymbol{\vartheta} = \boldsymbol{\theta}_{(2)}^{*\top} (\mathbf{C}_{22} - \mathbf{C}_{21} \mathbf{C}_{11}^{-1} \mathbf{C}_{12}) \boldsymbol{\theta}_{(2)}^*$. \square

Finally, the following elementary lemma provides a useful technical tool for simplifying some of the algebraic inequalities:

Lemma 4. *The quadratic function $f(x) = ax^2 - bx - c$ with $a, b, c > 0$ is positive for all real x satisfying*

$$x^2 \geq \left(\frac{b}{a}\right)^2 + 2\frac{c}{a}.$$

Proof. Clearly, $f(x)$ has only one positive root, denoted here by x_+ , which satisfies $f(x) > 0, \forall x > x_+$. Using the following instance of Jensen's inequality,

$$\sqrt{1+z} \leq \frac{1}{2}z + 1 \quad \forall z > 0,$$

the positive root x_+ can be upper bounded as:

$$\begin{aligned} x_+^2 &= \left(\frac{b}{2a} + \sqrt{\left(\frac{b}{2a}\right)^2 + \frac{c}{a}}\right)^2 \\ &= 2\left(\frac{b}{2a}\right)^2 + \frac{c}{a} + 2\frac{b}{2a}\sqrt{\left(\frac{b}{2a}\right)^2 + \frac{c}{a}} \\ &\leq 2\left(\frac{b}{2a}\right)^2 + \frac{c}{a} + 2\left(\frac{b}{2a}\right)^2 \left(\frac{1}{2}\left(\frac{2a}{b}\right)^2 \frac{c}{a} + 1\right) \\ &= \left(\frac{b}{a}\right)^2 + 2\frac{c}{a} = x_0^2 \end{aligned}$$

Then, $x^2 \geq x_0^2$ implies $ax^2 - bx - c > 0$. □

ACKNOWLEDGMENT

The authors would like to thank Patrick L. Purdon and Emery N. Brown for providing the data from [66].

REFERENCES

- [1] W. H. Greene, *Econometric Analysis*. The address: Pearson Education, Inc., Upper Saddle River, New Jersey, 07458, 5th ed., 2003.
- [2] S. L. Bressler and A. K. Seth, "Wiener-Granger causality: A well established methodology," *Neuroimage*, vol. 58, no. 2, pp. 323–329, 2011.
- [3] K. Friston, R. Moran, and A. K. Seth, "Analysing connectivity with Granger causality and dynamic causal modelling," *Curr. Opin. Neurobiol.*, vol. 23, no. 2, pp. 172–178, 2013.
- [4] A. K. Seth, A. B. Barrett, and L. Barnett, "Granger Causality Analysis in Neuroscience and Neuroimaging," *J. Neurosci.*, vol. 35, no. 8, pp. 3293–3297, 2015.
- [5] E. Klipp, R. Herwig, A. Kowald, C. Wierling, and H. Lehrach, *Systems biology in practice: concepts, implementation and application*. John Wiley & Sons, 2005.
- [6] J. Feng, J. Jost, and M. Qian, *Networks: from biology to theory*, vol. 80. Springer, 2007.
- [7] C. W. J. Granger, "Investigating Causal Relations by Econometric Models and Cross-spectral Methods," *Econometrica*, vol. 37, no. 3, pp. 424–438, 1969.
- [8] J. Geweke, "Measurement of linear dependence and feedback between multiple time series," *J. Am. Stat. Assoc.*, vol. 77, no. 378, pp. 304–313, 1982.
- [9] J. F. Geweke, "Measures of Conditional Linear Dependence and Feedback Between Time Series," *J. Am. Stat. Assoc.*, vol. 79, no. 388, pp. 907–915, 1984.
- [10] I. E. Marinescu, P. N. Lawlor, and K. P. Kording, "Quasi-experimental causality in neuroscience and behavioural research," *Nature human behaviour*, vol. 2, no. 12, pp. 891–898, 2018.
- [11] J. Pearl, *Causality*. Cambridge university press, 2009.
- [12] H. Akaike, "A new look at the statistical model identification," *IEEE Trans. Autom. Control*, vol. 19, no. 6, pp. 716–723, 1974.

- [13] G. Schwarz, “Estimating the Dimension of a Model,” *Ann. Stat.*, vol. 6, no. 2, pp. 461–464, 1978.
- [14] S. Kim, D. Putrino, S. Ghosh, and E. N. Brown, “A Granger causality measure for point process models of ensemble neural spiking activity,” *PLoS Comput. Biol.*, vol. 7, no. 3, 2011.
- [15] A. Wald, “Tests of Statistical Hypotheses Concerning Several Parameters When the Number of Observations is Large,” *Trans. Am. Math. Soc.*, vol. 54, no. 3, pp. 426–482, 1943.
- [16] R. R. Davidson and W. E. Lever, “The Limiting Distribution of the Likelihood Ratio Statistic under a Class of Local Alternatives,” *Sankhyā Indian J. Stat. Ser. A*, vol. 32, no. 2, pp. 209–224, 1970.
- [17] C. Zou and J. Feng, “Granger causality vs. dynamic Bayesian network inference: a comparative study,” *BMC Bioinformatics*, vol. 10, no. 1, p. 122, 2009.
- [18] A. K. Seth, “A MATLAB toolbox for Granger causal connectivity analysis,” *J. Neurosci. Methods*, vol. 186, no. 2, pp. 262–273, 2010.
- [19] P. P. Mitra and B. Pesaran, “Analysis of dynamic brain imaging data,” *Biophys. J.*, vol. 76, no. 2, pp. 691–708, 1999.
- [20] M. T. Bahadori and Y. Liu, “An examination of practical Granger causality inference,” in *Proc. 2013 SIAM Int. Conf. data Min.*, pp. 467–475, SIAM, 2013.
- [21] A. Goldenshluger and A. Zeevi, “Nonasymptotic Bounds for Autoregressive Time Series Modeling,” *Ann. Stat.*, vol. 29, pp. 417–444, Mar 2001.
- [22] H. Wang, G. Li, and C.-L. Tsai, “Regression coefficient and autoregressive order shrinkage and selection via the lasso,” *J. R. Stat. Soc. Ser. B (Statistical Methodol.)*, vol. 69, no. 1, pp. 63–78, 2007.
- [23] Y. Nardi and A. Rinaldo, “Autoregressive process modeling via the Lasso procedure,” *J. Multivar. Anal.*, vol. 102, no. 3, pp. 528–549, 2011.
- [24] F. Han and H. Liu, “Transition matrix estimation in high dimensional time series,” in *Int. Conf. Mach. Learn.*, pp. 172–180, 2013.
- [25] A. Kazemipour, S. Miran, P. Pal, B. Babadi, and M. Wu, “Sampling requirements for stable autoregressive estimation,” *IEEE Trans. Signal Process.*, vol. 65, no. 9, pp. 2333–2347, 2017.
- [26] S. Basu, G. Michailidis, and Others, “Regularized estimation in sparse high-dimensional time series models,” *Ann. Stat.*, vol. 43, no. 4, pp. 1535–1567, 2015.
- [27] K. C. Wong, Z. Li, and A. Tewari, “Lasso guarantees for β -mixing heavy-tailed time series,” *Ann. Stat.*, vol. 48, no. 2, pp. 1124–1142, 2020.
- [28] A. Skripnikov and G. Michailidis, “Regularized joint estimation of related vector autoregressive models,” *Comput. Stat. Data Anal.*, vol. 139, pp. 164–177, 2019.
- [29] S. Basu, X. Li, and G. Michailidis, “Low Rank and Structured Modeling of High-Dimensional Vector Autoregressions,” *IEEE Trans. Signal Process.*, vol. 67, no. 5, pp. 1207–1222, 2019.
- [30] R. Tibshirani, “Regression Shrinkage and Selection Via the Lasso,” *J. R. Stat. Soc. Ser. B*, vol. 58, no. 1, pp. 267–288, 1996.
- [31] P.-L. Loh and M. J. Wainwright, “High-dimensional regression with noisy and missing data: Provable guarantees with non-convexity,” in *Adv. Neural Inf. Process. Syst.* 24, pp. 2726–2734, 2011.
- [32] S. N. Negahban, P. Ravikumar, M. J. Wainwright, and B. Yu, “A Unified Framework for High-Dimensional Analysis of M -Estimators with Decomposable Regularizers,” *Stat. Sci.*, vol. 27, no. 4, pp. 538–557, 2012.
- [33] T. Hastie, R. Tibshirani, and M. Wainwright, *Statistical learning with sparsity: the lasso and generalizations*. CRC press, 2015.
- [34] N.-J. Hsu, H.-L. Hung, and Y.-M. Chang, “Subset selection for vector autoregressive processes using Lasso,” *Comput. Stat. Data Anal.*, vol. 52, no. 7, pp. 3645–3657, 2008.
- [35] Y. Ren and X. Zhang, “Subset selection for vector autoregressive processes via adaptive Lasso,” *Stat. Probab. Lett.*, vol. 80, no. 23, pp. 1705–1712, 2010.
- [36] Y. Ren and X. Zhang, “Model selection for vector autoregressive processes via adaptive Lasso,” *Commun. Stat. Methods*, vol. 42, no. 13, pp. 2423–2436, 2013.
- [37] A. Arnold, Y. Liu, and N. Abe, “Temporal causal modeling with graphical granger methods,” in *Proc. 13th ACM SIGKDD Int. Conf. Knowl. Discov. data Min.*, pp. 66–75, 2007.
- [38] A. C. Lozano, N. Abe, Y. Liu, and S. Rosset, “Grouped graphical Granger modeling for gene expression regulatory networks discovery,” *Bioinformatics*, vol. 25, no. 12, pp. i110–i118, 2009.
- [39] A. Shojaie and G. Michailidis, “Discovering graphical Granger causality using the truncating lasso penalty,” *Bioinformatics*, vol. 26, no. 18, pp. i517–i523, 2010.

- [40] Y. Liu, M. T. Bahadori, and H. Li, “Sparse-gev: Sparse latent space model for multivariate extreme value time series modeling,” in *Proc. 29th Int. Conf. Mach. Learn. Edinburgh, Scotland, UK*, 2012.
- [41] S. Basu, A. Shojaie, and G. Michailidis, “Network Granger Causality with Inherent Grouping Structure,” *J. Mach. Learn. Res.*, vol. 16, no. 1, pp. 417–453, 2015.
- [42] G. Michailidis and F. D’Alché-Buc, “Autoregressive models for gene regulatory network inference: Sparsity, stability and causality issues,” *Math. Biosci.*, vol. 246, no. 2, pp. 326–334, 2013.
- [43] A. Tank, I. Covert, N. Foti, A. Shojaie, and E. Fox, “Neural granger causality for nonlinear time series,” *arXiv preprint arXiv:1802.05842*, 2018.
- [44] P. Bühlmann and S. Van De Geer, *Statistics for high-dimensional data: methods, theory and applications*. Berlin: Springer Science & Business Media, 2011.
- [45] W. Tang, S. L. Bressler, C. M. Sylvester, G. L. Shulman, and M. Corbetta, “Measuring Granger causality between cortical regions from voxelwise fMRI BOLD signals with LASSO,” *PLoS Comput. Biol.*, vol. 8, no. 5, 2012.
- [46] S. van de Geer, P. Bühlmann, Y. Ritov, and R. Dezeure, “On asymptotically optimal confidence regions and tests for high-dimensional models,” *Ann. Stat.*, vol. 42, no. 3, pp. 1166–1202, 2014.
- [47] S. van de Geer, “On the asymptotic variance of the debiased Lasso,” *Electron. J. Stat.*, vol. 13, no. 2, pp. 2970–3008, 2019.
- [48] A. Javanmard and A. Montanari, “Confidence Intervals and Hypothesis Testing for High-Dimensional Regression,” *J. Mach. Learn. Res.*, vol. 15, no. 1, pp. 2869–2909, 2014.
- [49] A. Javanmard, A. Montanari, and Others, “Debiasing the lasso: Optimal sample size for gaussian designs,” *Ann. Stat.*, vol. 46, no. 6A, pp. 2593–2622, 2018.
- [50] A. Javanmard, H. Javadi, and Others, “False discovery rate control via debiased lasso,” *Electron. J. Stat.*, vol. 13, no. 1, pp. 1212–1253, 2019.
- [51] M. Dhamala, G. Rangarajan, and M. Ding, “Analyzing information flow in brain networks with nonparametric Granger causality,” *Neuroimage*, vol. 41, no. 2, pp. 354–362, 2008.
- [52] I. Vlachos and D. Kugiumtzis, “Nonuniform state-space reconstruction and coupling detection,” *Phys. Rev. E*, vol. 82, p. 16207, Jul 2010.
- [53] J. Runge, S. Bathiany, E. Bollt, G. Camps-Valls, D. Coumou, E. Deyle, C. Glymour, M. Kretschmer, M. D. Mahecha, J. Muñoz-Marí, et al., “Inferring causation from time series in earth system sciences,” *Nature communications*, vol. 10, no. 1, pp. 1–13, 2019.
- [54] J. Runge, P. Nowack, M. Kretschmer, S. Flaxman, and D. Sejdinovic, “Detecting and quantifying causal associations in large nonlinear time series datasets,” *Science Advances*, vol. 5, no. 11, p. eaau4996, 2019.
- [55] J. Runge, V. Petoukhov, J. F. Donges, J. Hlinka, N. Jajcay, M. Vejmelka, D. Hartman, N. Marwan, M. Paluš, and J. Kurths, “Identifying causal gateways and mediators in complex spatio-temporal systems,” *Nature communications*, vol. 6, no. 1, pp. 1–10, 2015.
- [56] G. H. Golub, P. C. Hansen, and D. P. O’Leary, “Tikhonov Regularization and Total Least Squares,” *SIAM J. Matrix Anal. Appl.*, vol. 21, no. 1, pp. 185–194, 1999.
- [57] F. Natterer, “Error bounds for Tikhonov regularization in Hilbert scales,” *Appl. Anal.*, vol. 18, no. 1-2, pp. 29–37, 1984.
- [58] J. Fan and R. Li, “Variable selection via nonconcave penalized likelihood and its oracle properties,” *J. Am. Stat. Assoc.*, vol. 96, no. 456, pp. 1348–1360, 2001.
- [59] H. Xie and J. Huang, “SCAD-penalized regression in high-dimensional partially linear models,” *Ann. Stat.*, vol. 37, no. 2, pp. 673–696, 2009.
- [60] H. Zou and T. Hastie, “Regularization and variable selection via the elastic net,” *J. R. Stat. Soc. Ser. B (statistical Methodol.)*, vol. 67, no. 2, pp. 301–320, 2005.
- [61] P. Zhao and B. Yu, “On model selection consistency of Lasso,” *J. Mach. Learn. Res.*, vol. 7, pp. 2541–2563, 2006.
- [62] J. Ding, V. Tarokh, and Y. Yang, “Model Selection Techniques: An Overview,” *IEEE Signal Process. Mag.*, vol. 35, pp. 16–34, Nov 2018.
- [63] H. Lütkepohl, *New introduction to multiple time series analysis*. Springer-Verlag, Berlin, 2005.
- [64] T. Goldstein and S. Osher, “The Split Bregman Method for L1-Regularized Problems,” *SIAM J. Imaging Sci.*, vol. 2, no. 2, pp. 323–343, 2009.
- [65] L. D. Lewis, S. Ching, V. S. Weiner, R. A. Peterfreund, E. N. Eskandar, S. S. Cash, E. N. Brown, and P. L. Purdon, “Local cortical dynamics of burst suppression in the anaesthetized brain,” *Brain*, vol. 136, no. 9, pp. 2727–2737, 2013.
- [66] L. D. Lewis, V. S. Weiner, E. A. Mukamel, J. A. Donoghue, E. N. Eskandar, J. R. Madsen, W. S. Anderson, L. R. Hochberg, S. S. Cash, E. N. Brown, and P. L. Purdon, “Rapid fragmentation of neuronal networks at the onset of propofol-induced unconsciousness,” *Proc. Natl. Acad. Sci.*, vol. 109, no. 49, pp. E3377–E3386, 2012.

- [67] S. Chauvette, S. Crochet, M. Volgushev, and I. Timofeev, “Properties of slow oscillation during slow-wave sleep and anesthesia in cats,” *J. Neurosci.*, vol. 31, no. 42, pp. 14998–15008, 2011.
- [68] B. O. Watson, D. Levenstein, J. P. Greene, J. N. Gelin, and G. Buzsáki, “Network Homeostasis and State Dynamics of Neocortical Sleep,” *Neuron*, vol. 90, no. 4, pp. 839–852, 2016.